Sedimentology (2020) doi: 10.1111/sed.12775

Geochemical fingerprints of dolomitization in Bahamian carbonates: Evidence from sulphur, calcium, magnesium and clumped isotopes

SEAN T. MURRAY *,1 , JOHN A. HIGGINS † , CHRIS HOLMDEN ‡ , CHAOJIN LU * and PETER K. SWART *

*Department of Marine Geoscience, Rosenstiel School of Marine and Atmospheric Sciences, University of Miami, 4600 Rickenbacker Causeway, Miami, FL, 33149, USA (E-mail: pswart@rsmas.miami.edu) †Department of Earth Sciences, Princeton University, Princeton, NJ, 08544, USA ‡Department of Geological Sciences, University of Saskatchewan, Saskatoon, SK, S7N 5E2, Canada

Associate Editor - Cathy Hollis

ABSTRACT

In an effort to constrain the mechanism of dolomitization in Neogene dolomites in the Bahamas and improve understanding of the use of chemostratigraphic tracers in shallow-water carbonate sediments the δ^{34} S, Δ_{47} , δ^{13} C, δ^{18} O, $\delta^{44\tilde{1}40}$ Ca and δ^{26} Mg values and Sr concentrations have been measured in dolomitized intervals from the Clino core, drilled on the margin of Great Bahama Bank and two other cores (Unda and San Salvador) in the Bahamas. The Unda and San Salvador cores have massively dolomitized intervals that have carbonate associated sulphate $\delta^{34}S$ values similar to those found in contemporaneous seawater and $\delta^{44/40}$ Ca, δ^{26} Mg values, Sr contents and Δ_{47} temperatures (25 to 30°C) indicating relatively shallow dolomitization in a fluidbuffered system. In contrast, dolomitized intervals in the Clino core have elevated values of carbonate associated sulphate δ^{34} S values indicating dolomitization in a more sediment-buffered diagenetic system where bacterial sulphate reduction enriches the residual SO₄²⁻ in ³⁴S, consistent with high sediment Sr concentrations and low $\delta^{44/40}$ Ca and high δ^{26} Mg values. Only dolomites associated with hardgrounds in the Clino core have carbonate associated δ^{34} S values similar to seawater, indicating continuous flushing of the upper layers of the sediment by seawater during sedimentary hiatuses. This interpretation is supported by changes to more positive $\delta^{44/40}$ Ca values at hardground surfaces. All dolomites, whether they formed in an open fluid-buffered or closed sediment-buffered diagenetic system have similar δ^{26} Mg values suggesting that the HMC transformed to dolomite. The clumped isotope derived temperatures in the dolomitized intervals in Clino yield temperatures that are higher than normal, possibly indicating a kinetic isotope effect on dolomite Δ_{47} values associated with carbonate formation through bacterial sulphate reduction. The findings of this study highlight the utility of applying multiple geochemical proxies to disentangle the diagenetic history of shallow-water carbonate sediments and caution against simple interpretations of stratigraphic variability in these geochemical proxies as indicating changes in the global geochemical cycling of these elements in seawater.

¹Present address: Department of Earth and Environmental Sciences, Stable Isotope Laboratory, Macquarie University, 12 Wally's Walk, NSW, 2109, Australia

Keywords Ca and Mg isotopes, clumped isotopes, diagenesis, dolomite, sulphur isotopes.

INTRODUCTION

The Bahamas is a vast shallow-water carbonate producing platform that has been repeatedly subjected to the influences of sea-level change during the Miocene-Pleistocene (Kievman, 1996; Kievman, 1998). During the Pleistocene, the upper portion of the sedimentary succession was periodically exposed to meteoric diagenesis due to glacio-eustatic sea-level changes, while older sediments have only been affected by marine processes (Swart & Oehlert, 2019). Because modern sediments in the Bahamas are dominated by non-skeletal carbonates (Beach & Ginsburg, 1980; Reijmer et al., 2009), interest in their geochemistry and diagenesis is widespread among workers studying Earth's early history (Swart & Kennedy, 2012; Hardisty et al., 2017; Ahm et al., 2018; Chen et al., 2018; Higgins et al., 2018; Tissot et al., 2018; Dellinger et al., 2019; Liu et al., 2019). In addition, the presence of widespread dolomites in the shallow subsurface of the Bahamas provides an opportunity to study this important, but poorly understood diagenetic process, where the timing and biogeochemical processes that drive dolomitization can be more precisely characterized. This paper focuses primarily on the origin of disseminated and intermittent 'background' dolomite within the Pliocene-Miocene part of the sedimentary succession in the Bahamas, using a combination of geochemical parameters (δ^{34} S, Δ_{47} , δ^{13} C, δ^{18} O, $\delta^{44/40}$ Ca, δ^{26} Mg and Sr concentrations). The geochemical parameters have been used to understand the role of organic material oxidation $(\delta^{13}C, \delta^{18}O \text{ and } \delta^{34}S)$, the temperature of formation (Δ_{47} and δ^{18} O) and the open versus closed nature of the diagenetic system ($\delta^{44/40}$ Ca, δ^{26} Mg and Sr). The results are applicable to the interpretation of marine diagenesis of carbonates in general and for stratigraphic variations in the geochemical patterns of these proxies.

There are two principal types of Neogene dolomite occurrences in the Bahamas. These are: (i) massive dolomites (>95%) found in shallow water carbonate sediments; and (ii) a spatially limited and scattered background dolomite (<1% to ca 50%) in deeper water fine-grained to muddy carbonates. The massive dolomites are hypothesized to form as a result of subsurface

Mg-bearing fluid flow in an open diagenetic system (Vahrenkamp & Swart, 1994), while background dolomites form by advection and diffusion of Mg into sediments from overlying seawater (Mullins et al., 1985; Swart & Melim, 2000). In addition, dolomite has also been reported in tidal flats on Andros Island (Shinn et al., 1969) and some shallow hypersaline ponds, although these environments are not major locations of dolomite formation at the present time.

Many studies have described Pliocene and Miocene sections of carbonates in Little Bahama Bank, Great Bahama Bank (GBB), San Salvador and Mavaguana that have been completely dolomitized (Supko, 1977; Kaldi & Gidman, 1982; Pierson, 1983; Mullins et al., 1985; Dawans & Swart, 1988; Mullins et al., 1988; Vahrenkamp, 1988; Vahrenkamp et al., 1991; Vahrenkamp & Swart, 1994; Swart & Melim, 2000; Murray & Swart, 2017). These relatively young and massive dolomites are believed to have formed during periods of time when seawater flowed through parts of the carbonate succession under glacioeustatic sea-level control (Vahrenkamp et al., 1991; Swart & Melim, 2000). They are interpreted to have formed at close to equilibrium with modern seawater based on Sr concentrations (Vahrenkamp & Swart, 1990) and contain ⁸⁷Sr/⁸⁶Sr ratios similar to the depositional age of the sediment (Swart et al., 1987; Vahrenkamp et al., 1991) and are therefore likely to have formed in a seawaterbuffered open diagenetic system.

A second type of dolomite found in the Bahamas typically comprises a small proportion of deeper-water sedimentary deposits, generally <10%, but occasionally reaching 50%, associated with intervals of reduced sedimentation. Such 'background dolomites' are not only found in sedimentary rocks discovered in deeper water off the Bahamas (Mullins et al., 1985; Eberli et al., 1997a; Swart & Melim, 2000), but also associated with other carbonate platforms such as the Maldives (Betzler et al., 2016), Great Barrier Reef (Davies et al., 1991) and Great Australian Bight (Feary et al., 1998; Rivers et al., 2012) and along continental margins (Kelts & McKenzie, 1982). In the Bahamas, based on changes in δ^{13} C, δ^{18} O values and Sr concentrations, they have been interpreted to form in

response to the oxidation of organic material by bacterial sulphate reduction (BSR) with Mg²⁺ diffusing into the sediment from the base of the flushed zone (Eberli *et al.*, 1997a; Kramer *et al.*, 2000) or the dissolution of high-Mg calcite (HMC) (Swart & Melim, 2000). Higher concentrations of background dolomite are associated with numerous hardground surfaces in the core. These dolomites appear to have formed during periods of sediment starvation and increased exposure of sediments in the flush zone to advected supplies of reactive Mg.

SAMPLES

Samples were taken from three cores collected from the Bahamas: Clino and Unda located on the western margin of Great Bahama Bank and a third core from the island of San Salvador located on the eastern edge of the Bahamas platform (Fig. 1). The Clino and Unda cores were collected in a study designed to examine the timing and sedimentology of the prograding margin of the platform (Ginsburg, 2001). Detailed descriptions of these cores can be found in McNeill *et al.* (2001), Kenter *et al.* (2001), Eberli (2000), Swart & Melim

(2000) and Melim *et al.* (2004). Depths in both cores are reported in metres below the mud pit datum (mbmp), which is 14.9 m above sea level for Clino and 11.9 m for Unda. For this study, samples were collected throughout the Clino core for clumped and sulphur isotope analyses, while the San Salvador and Unda cores were sampled and analyzed only in the dolomitized intervals.

The Clino core (Fig. 2) penetrates 677.1 m of slope to upper slope deposits of a shallowing upward sequence of peloidal and skeletal wackestone or coral framestone (Kenter et al., 2001). The core can be separated into three distinct lithological layers: (i) an upper layer of reefal deposits and shallow water platform derived sediments (21.6 to 197.4 mbmp); (ii) a middle layer composed mostly of non-skeletal fine-grained sediments with periodic layers of skeletal material (197.4 to 367.04 mbmp); and (iii) a deep layer that is a mixture of skeletal and fine-grained nonskeletal sediments (367.04 to 677.27 mbmp). Dolomite first appears around 150 mbmp just below a transition from negative δ^{13} C and δ^{18} O values indicative of meteoric and mixing-zone diagenesis to positive values more expected of marine-burial diagenesis (Allan & Matthews, 1982; Eberli et al., 1997b; Swart, 2015). The

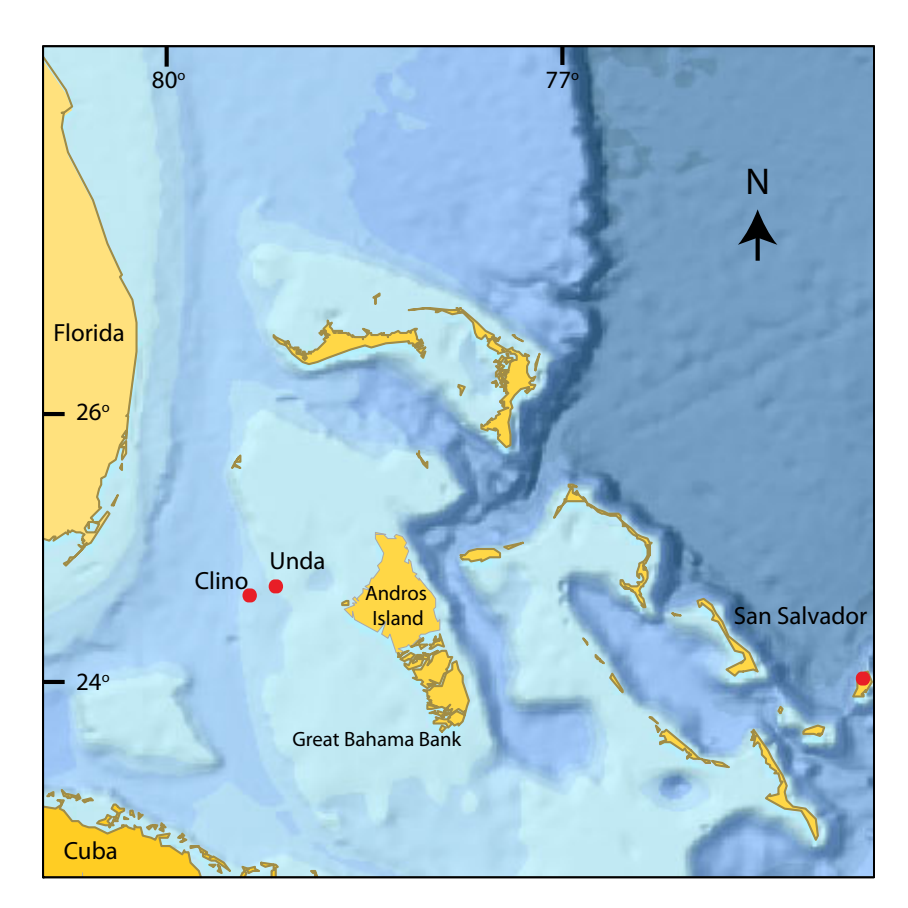


Fig. 1. Location of the cores investigated in this study.

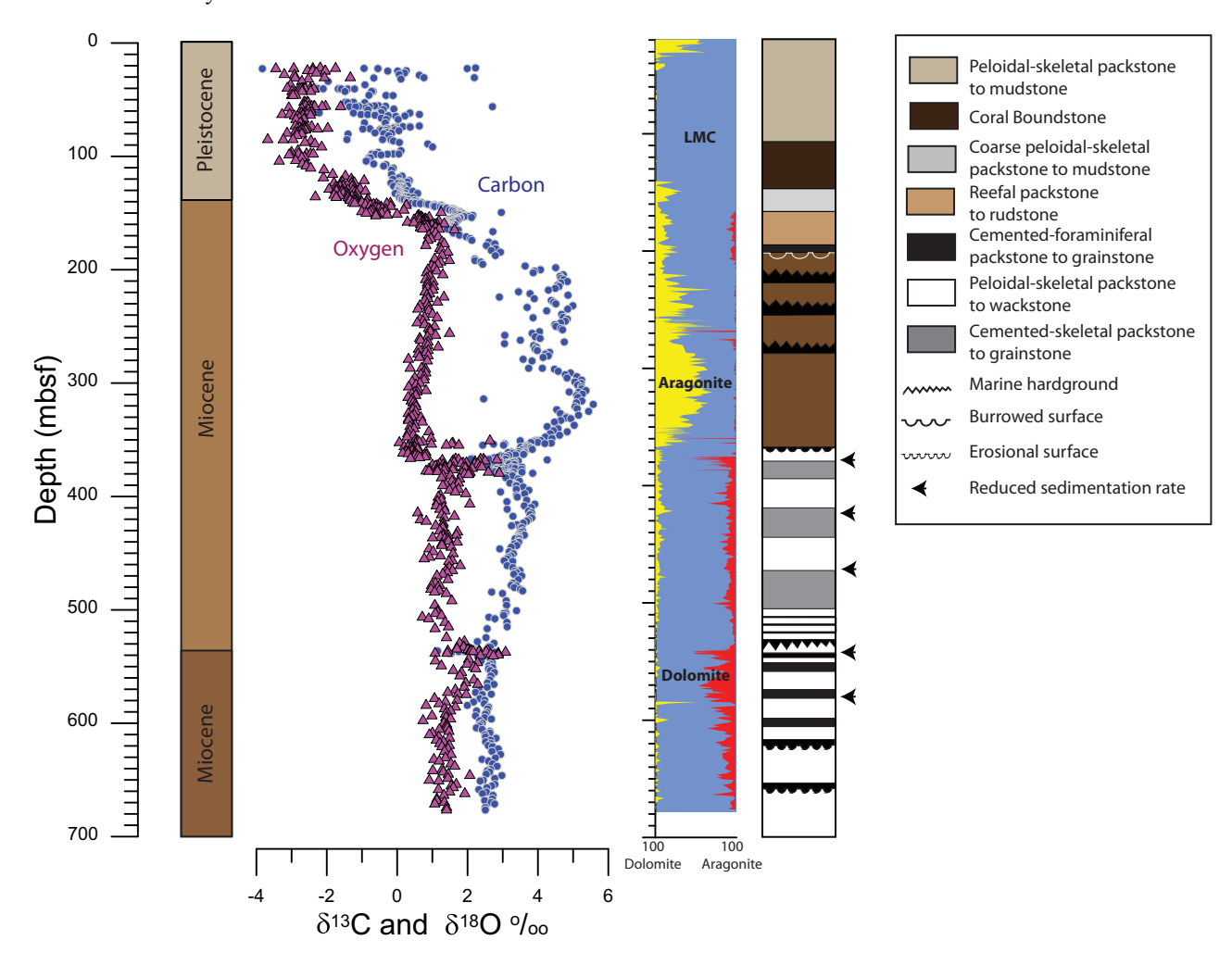


Fig. 2. Stratigraphy (McNeill *et al.*, 2001), mineralogy and stable C (blue circles) and O (purple triangles) isotope values from the Clino core (Melim *et al.*, 2001) compared to a summary of sedimentology and non-depositional surfaces (Kenter *et al.*, 2001).

greatest abundance of dolomite in the core is associated with marine hardgrounds reflecting hiatuses in carbonate sedimentation and/or submarine erosion of carbonate sediment, such as the erosional boundary at 367.04 m and the depositional hiatus at 536.33 mbmp (Fig. 3), but dolomite rarely exceeds more than 50% of the bulk composition and is typically much less. While the Mg/Ca ratio of the dolomites increases with increasing bulk percent dolomite, in all cases the dolomite remains calcian-rich, ranging from 41.8 to 45.8 mole % Mg, which is reflected in broadened 104-peaks obtained from X-ray diffraction (XRD) analysis (Swart & Melim, 2000). Petrographically, the dolomite present in Clino has varied textural forms ranging from fabric-preserving through micritic and isolated fine-grained

rhombs and fabric destructive microsucrosic (Swart & Melim, 2000), although commonly the dolomite is of an intermediate form. The fabric preserving dolomite is restricted to the most denselv dolomitized sections of the core, usually >80% bulk dolomite, which is consistently found in a blocky spar-cemented skeletal grainstone to packstone. Grains of red algae and Halimeda with an infilling blocky spar dolomite cement are easily recognized within these sections, often with a distinct pleochroism compared to surrounding dolomite cements. Most of the fabric preserving dolomite intervals also contain large euhedral rhombs of dolomite spar with luminescent rims under cathodoluminescence. Typically, these isolated rhombs are void filling and range from 1 to 40 µm in size in both deep-water facies

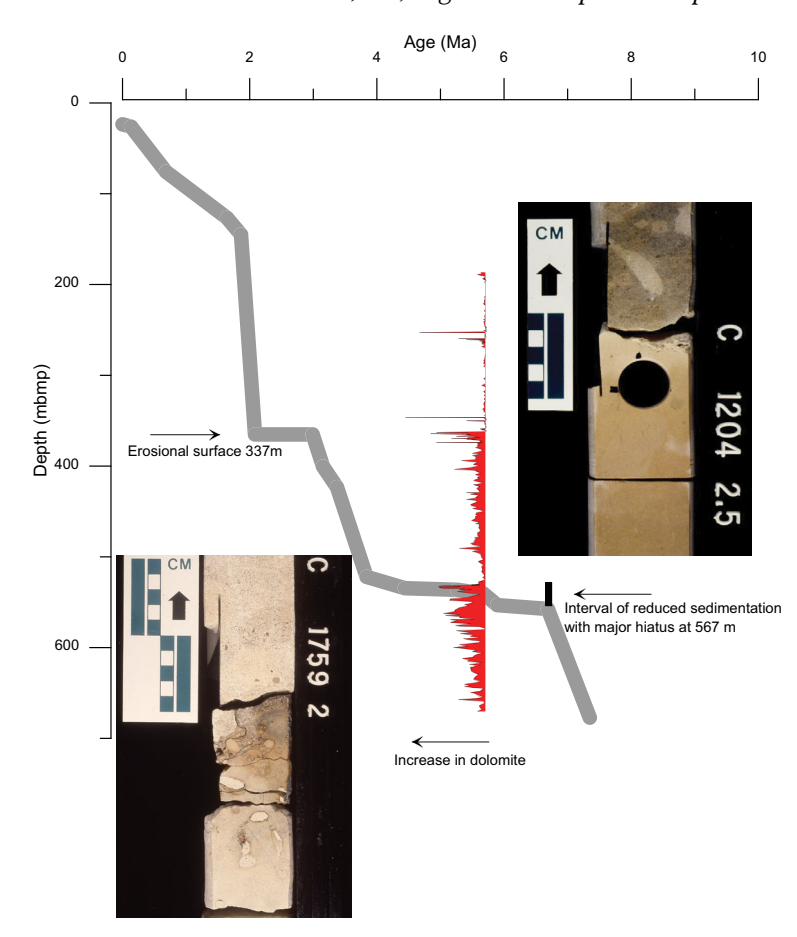


Fig. 3. Photographs of the erosional surface at 367 (1204'2.5") and hardground at 536 (1759'2") metres below the mud pit datum (mbmp) in the Clino core together with the integrated age model based on biostratigraphy, chemostratigraphy and magnetostratigraphy (McNeill et al., 2001). The abundance of dolomite from Fig. 2 is superimposed emphasizing the increasing concentrations associated with these two surfaces.

and in the upper sections of the core where dolomite is <5% of the modal mineralogy. At the nondepositional and erosional hardgrounds, a micritic dolomite replaces grains and acts as the lithifying cement. It is believed to have formed during hardground formation because it often overlays phosphatic crusts and because the abundance of dolomite decreases with depth below the surface of the hardground. Carbonate $\delta^{18}O$ values and Sr concentrations also increase below the hardground suggesting an evolution of pore fluid chemistry away from the hardground surface as dolomitization occurred. As a result of the association of dolomite with the hardgrounds, the timing of dolomitization is believed to be contemporaneous with the depositional hiatuses. This conclusion is further supported by Sr-isotope data which shows an abrupt shift in ⁸⁷Sr/⁸⁶Sr below the 536.33 m hardground that agrees with the biostratigraphic age of the sediments.

Based on the geological and diagenetic evidence, clumped isotope temperatures are expected to reflect dolomite formation from Bahamian surface seawater at temperatures of *ca*

20 to 30°C, or slightly lower water temperatures of ca 10 to 20°C for deeper water sediment deposited on the slope of the Bahamas margin. In total, 42 bulk carbonate samples spanning the length of the core were measured for clumped isotopes and 45 were measured for δ^{34} S values in carbonate associated sulphate (CAS).

Core Unda was drilled along the same seismic line as Clino, but 8.5 km onto the platform penetrating 454.15 mbmp (Ginsburg, 2001). The sediments of Unda are comprised mostly of reefal buildups and platform derived sediments with some deeper marginal deposits towards the bottom of the core (Kenter et al., 2001). Trace amounts of dolomite first occur below 108.1 mbmp with increasing abundances (up to 80%, but typically 20 to 40%) from 108 to 235 mbmp and 354 to 452 mbmp depth. From 292 to 360 mbmp, just below the Miocene-Pliocene boundary, an interval of platform to middle-reef sediments is 100% dolomitized. Budd & Manfrino (2001) examined the fauna that produced the now dolomitized reef and suggested that it originally formed in waters as deep as 20 to 40 m, indicating that ca 300 m of subsidence has occurred over ca 5.33 Myr. The carbonate sediment in the upper 108 m of the core exhibits negative δ^{13} C and δ^{18} O values (δ^{13} C = -1.6%, $1\sigma = 1.7\%$, $\delta^{18}O = -3.0\%$, $1\sigma = 0.7\%$, $\pm 1\sigma$), while the sediment below this level exhibits only positive values ($\delta^{13}C = 3.0\%$, $1\sigma = 0.9\%$; $\delta^{18}O = 0.9\%$, $1\sigma = 0.3\%$ and 3.4%, $1\sigma = 0.3\%$, for calcite and dolomite, respectively) (Melim et al., 2001). This downcore change in stable C and O isotope values signifies a change from meteoric diagenesis to marine diagenesis. Twelve samples from Unda, primarily from within the completely dolomitized reefal interval in the lower part of the core, were analyzed for δ^{34} S values in CAS.

The San Salvador (Fig. 1) core extends 168 m through Pleistocene to Miocene aged carbonate sediments. The age of the sediments was determined through a combination of biostratigraphy, Sr-isotope stratigraphy (Swart et al., 1987) and magnetostratigraphy (McNeill et al., 1988). A 110 m interval, from 35 to 145 m depth in the core, is composed entirely of well-ordered, near stoichiometric (43 to 50% MgCO₃) dolomite (Supko, 1977). The rest of the core is composed predominantly of low-Mg calcite (LMC). For this study, 24 samples from the dolomitized sections were analyzed for their CAS δ^{34} S values. Clumped isotope values from both Unda and San Salvador were measured by Murray & Swart (2017).

GEOCHEMICAL DATA

There have been a number of geochemical studies of these cores. These workers and the elements and isotopes they studied are summarized in Table 1 and will be incorporated into the *Discussion* as appropriate. In particular the Sr concentration data presented by Swart & Melim (2000) (Clino and Unda), Dawans & Swart (1988) (San Salvador) and the Ca and Mg isotope data (Clino and Unda) presented by Higgins *et al.* (2018) will be used. All relevant analytical techniques are provided in these referenced papers.

METHODS

X-ray diffraction

Samples were powdered and subject to X-ray diffraction using a Panalytical X-Pert Pro (Malvern Panalytical Limited, Malvern, UK)

Table 1. Summary of previous geochemical work on the three cores studied.

	Clino	Unda	San Salvador
C and O isotopes	1, 2, 7, 17, 18	1, 2, 7	4, 5
Organic C	3	_	_
Trace elements (Fe, I, Sr, Mg)	6, 7	6, 7	4, 5, 14
REE	15	_	_
U-isotopes	8	8	_
Ca and Mg isotopes	9	9	_
Clumped isotopes	_	10	10
Sr-isotopes	11	11	12, 13
Li-isotopes	16	_	_

1 - Melim et al. (1995); 2 - Melim et al. (2001); 3 - Oehlert & Swart (2014); 4 - Supko (1977); 5 - Dawans & Swart (1988); 6 - Kievman (1998); 7 - Hardisty et al. (2017); 8 - Chen et al. (2018); 9 - Higgins et al. (2018); 10 - Murray & Swart (2017); 11 - Swart et al. (2001); 12 - Swart et al. (1987); 13 - Vahrenkamp et al. (1991); 14 - Swart (1988); 15 - Liu et al. (2019); 16 - Murphy et al. (2018); 17 - Swart & Oehlert (2019); 18 - Oehlert & Swart (2019).

with copper radiation. In order to determine the abundance of dolomite the samples were scanned between 23° and 32° 2θ using a step interval of 0.01° and a count time of 1 s per step. The percentage of dolomite was then quantified using the peak areas and calibrated using a set of six standards employing the method described by Swart *et al.* (2002). Peak ordering was determined by scanning the samples between 20° and 55° 2θ using a step interval of 0.02° and a count time of 1 s per step.

Carbonate associated sulphate

Preparation of the CAS samples followed the methods of Gill et al. (2011). Samples for CAS analysis were obtained by freshly cutting large chips out of the individual cores. Samples were powdered using short intervals in a Spex SamplePrep Mixer/Mill 8000 (SPEX® SamplePrep, Metuchen, NJ, USA). Each CAS sample consisted of 20 to 30 g of powdered sample which was soaked in a 10% NaCl solution for 24 h followed by two consecutive rinses with DI water lasting 24 h. This was followed by a 4% sodium hypochlorite solution soak for 48 h to

remove any organically formed sulphur compounds. Two 24-h DI water rinses were then applied before the samples were dissolved using a 4 N hydrochloric acid solution. Upon complete dissolution of all carbonate material, any undissolved portions of the sample were removed from the supernatant via vacuum filtering through 45 µm glass microfibre filters. The filtered supernatant was then added to 100 ml of a saturated BaCl₂ solution (250 g l^{-1}), brought up to 1 l total volume through the addition of DI water and allowed to settle and precipitate for three days. The precipitate was then removed from the remaining solution and dried over 72 h in a 40°C oven before being sampled for analysis. If the dried samples contained evidence of crystallized hydrochloric acid, they were re-dissolved in a litre of DI water, allowed to settle overnight then recollected and dried. The second treatment was sometimes necessary as the beaker volume (1 l) was often not large enough to dilute the concentrated hydrochloric acid solution sufficiently to remove all traces of the acid. It is not believed that this additional step introduced any fractionation of sulphur isotopes in the samples, but this step did significantly improve the quality of samples that showed evidence of impurities from the hydrochloric acid.

The CAS sample analysis consisted of 1 mg of BaSO₄ sample combined with 5 mg of vanadium-pentoxide (V₂O₅) in a single tin capsule. The tin capsules were combusted in a modified Dumas group combustion furnace (Europa Scientific). The resulting SO₂ gas was analyzed using a continuous flow isotope ratio mass spectrometer (Europa Scientific, Crewe, UK). In order to homogenize the oxygen value in the SO₂, the gas was passed over quartz chips heated to 1000°C (Fry et al., 2002). The δ^{34} S value was determined by the measurement of masses 50 and 48 and was corrected to three different standards: an in-house standard calibrated to Vienna Canyon Diablo Troilite (V-CDT) and two IAEA (International Atomic Energy Agency) standards, (National Bureau of Standards) NBS 123, a seawater sulphate and NBS 127, a sphalerite. Between each sample and standard, a single blank was measured to make sure that the sulphur from the previous sample had completely flushed through the system. Sample δ^{34} S values are reported relative to V-CDT. As a result of sample size limitations for CAS, the samples used for clumped isotopes were not always the same samples used for CAS

measurements. A linear drift correction was applied to each run of CAS samples by measuring a complete set of all three in-house standards before and after the run with a single standard measured in the middle of the run. The amount of drift typically averaged 3% to 10% of the isotopic value of the standard. Based on the analysis of replicate samples and the single standard interspersed in the middle of the run, the precision on these measurements averaged to 0.6, $1\sigma = 0.6\%$.

Isolation of the dolomite

As the sediments from Clino are partially dolomitized, in order to understand the contribution that each end member contributes to the clumped isotope signal, bulk samples were treated using a buffered glacial acetic acid to remove the less stable aragonite, calcite and VHMC phases, leaving only the most stable dolomite phase following the methods described in Swart & Melim (2000). Samples were mechanically ground and sifted to <63 µm in size. Approximately 75% of the total mass of the <63 µm fraction was then placed in a beaker (typically between 10 g and 20 g of sediment) and 30 ml of the acetic acid solution was then added. The samples were stirred for 2 to 3 h using a magnetic stir bar before being rinsed multiple times with DI water and set to dry in the 40°C oven over night. This process was repeated two to three times per sample until only the most stable carbonate phases remained. Bulk dolomite composition of these iterative treatments was determined using XRD and typically resulted in samples that were 90 to 100% dolomite after two to three washes. Unfortunately, this process did not lend itself to measuring the δ^{34} S value of the dolomite end member as the process dissolved too much sample, making the technique used to purify and concentrate S impractical for CAS isotopic analysis. In order to test the effects of this treatment on clumped isotope and C and O isotope analyses measurements, a laboratory standard (Carrara marble) composed of 100% LMC was mixed with a dolomite (NIST 88b) to create a mixture of 40% dolomite and 60% LMC. The resultant material was subjected to the separation procedure and the Δ_{47} , $\delta^{13}C$ and $\delta^{18}O$ values determined in the standard manner. These materials are ideal for this test because they have different original Δ_{47} , δ^{13} C and δ^{18} O values and therefore test the effectiveness of the procedure.

Clumped isotopes

Clumped isotope samples were measured over multiple measurement periods between 2013 and 2016. Each sample consisted of 8 to 10 mg of powder split between two K1250A 3.71 mm diameter gas check plain copper-boats which were subsequently loaded into a sample carousel that sits above a common acid bath that is connected to a high vacuum, stainless-steel processing line described in detail in Murray et al. (2016). Samples were digested over 30 to 60 min in 105% phosphoric acid (H₃PO₄) held at 90°C and constantly stirred by a PyrexTM coated magnetic stirbar with the length of reaction increasing with increased bulk percent dolomite of the sample. The produced CO₂ was cleaned by passing through a series of traps to remove water and a Utrap filled with Porapak[™] Type Q 50 to 80 mesh packing material before being manually transferred to a Thermo MAT 253 mass spectrometer (Thermo Fisher Scientific Inc., Waltham, MA, USA) in a removable sealed collection vessel.

Samples were measured against a cryogenically purified in-house reference gas (RG) calibrated against NBS 19 and reported relative to V-PDB. Over the course of this work, the RG was replaced once, in February of 2015 (RG1: $\delta^{13}C = -2.7\%$, $\delta^{18}O = -6.4\%$, RG2: $\delta^{13}C = -9.8\%$, $\delta^{18}O = -7$. 4%). The extracted signal was balanced to 12 V on mass 44. The δ^{13} C and δ^{18} O values are produced by simultaneously measuring masses 44, 45 and 46 and correcting for the typical isobaric interferences including acid digestion fractionation on δ^{18} O values using the fractionation factor of 1.0795 (Swart et al., 1991). In addition, the δ^{18} O values of the samples which contained >90% the dolomite were corrected for the differential fractionation of dolomite relative to calcite during the dissolution by phosphoric acid using an additional correction factor of -0.8% (Land, 1980).

Prior to August of 2014, samples were measured over ten acquisitions of six on-peak standard-sample reference measurements (click-clacks). After August of 2014, the pressure baseline (PBL) correction, as described in He *et al.* (2012), which has now become the norm for measurement of clumped isotopes on a MAT 253 mass spectrometer (Thermo Fisher Scientific Inc.) was implemented. The PBL measurements were performed with six acquisitions of fifteen on-peak click-clacks that were preceded and succeeded by five off-peak click-clacks measuring the background of the different mass voltages on the mass spectrometer. As shown in Murray *et al.* (2016), no

statistically significant differences in Δ_{47} values were produced by changing measurement methods. To check for long-term stability in the measurements of Δ_{47} values, an in-house Carrara marble standard was measured daily prior to any sample measurements and compared to accepted values (Dennis *et al.*, 2011).

The raw Δ_{47} values were calculated following the methods described by Huntington et al. (2009) using the ¹⁷O correction values suggested by Brand et al. (2010), based on recommendations from within the clumped isotope community (Daeron et al., 2016; Schauer et al., 2016). These parameters have been used despite the fact that when using equilibrated gases herein only minimal differences were found using the Brand et al. (2010) values compared to the values based on Craig (1957). The raw Δ_{47} values are converted to an absolute reference frame following the guidelines described in Dennis et al. (2011). Gas standards were created using four different CO_2 gases with a range of δ^{47} values and equilibrated either in sealed quartz tubes at 1000°C or in sealed Pyrex© tubes over deionized water at either 25°C or 50°C. The range in δ^{47} values of these gases is generated both by variations in the ¹³C/¹²C and ¹⁸O/¹⁶O ratios, unlike laboratories which use a single CO2 gas which is then equilibrated with waters of varying δ^{18} O values. The gas standards were produced and cleaned on the same vacuum line using the same methods as for the carbonate samples.

Some samples are mixtures of calcite, aragonite and dolomite. While work by Murray et~al.~(2016) and Müller et~al.~(2016) has suggested that dolomites have a significantly different acid digestion fractionation factor than calcite and aragonite with respect to Δ_{47} measurements (ca~0.13 to 0.153‰), in this study an equation generated in-house which was produced by reacting synthetically produced carbonates at 90°C (Staudigel et~al.,~2018) has been used. Therefore, a correction is not required and the data in this paper are not corrected for the acid fractionation factor between 25°C and 90°C. The equation proposed by Staudigel et~al.~(2018) and modified by Swart et~al.~(2019) for reaction at 90°C is used in this paper:

$$\begin{array}{ll} \Delta_{47} &= 0.0393(\pm.0017)*10^6/T^2 + 0.158(\pm.0088) \\ & \left(R^2 = 0.98\right) \end{array} \eqno(1)$$

Fluid compositions are calculated using the clumped isotope temperature and the calibrations of Kim & O'Neil (1997) for calcite and Matthews & Katz (1977) for dolomite using a linear mixing

model based on the bulk percent dolomite in each sample as determined from XRD. The Matthews & Katz (1977) equation was chosen in preference to a more recent equation by Horita (2014) because it provides more realistic values for fluids in other studies (Murray & Swart, 2017). Finally, the data presented in this paper were generated during a period of inter-laboratory testing using the ETH (Eidgenössische Technische Hochschule) (Bernasconi et al., 2018) standards (1 to 4). The data on these standards measured at this time are included in the Appendix S1 and are consistent with values reported by other laboratories. More comprehensive analysis of these standards measured during 2018 to 2019 are included in Swart et al. (2019).

Calcium and magnesium isotopes

Carbonate samples were dissolved in dilute ${\rm HNO_3}$ acid. The ${\rm Mg^{2+}}$ and ${\rm Ca^{2+}}$ ions were separated and purified from matrix elements using an automated ion chromatography (IC) system (Blättler et al., 2015) and analyzed for $\delta^{44/40}$ Ca and δ^{26} Mg values using a Thermo Scientific Neptune Plus multi-collector inductively-coupled plasma mass spectrometer (MC-ICP-MS) at Princeton. Sample-standard bracketing is used to correct for instrumental mass fractionation (Galy et al., 2001). The $\delta^{44/42}$ Ca values are converted to $\delta^{44/40}$ Ca values using the kinetic isotope fractionation law in which the ratio of ⁴⁴Ca/⁴²Ca is equal to the ratio of ⁴⁴Ca/⁴⁰Ca times 0.488 (Holmden et al., 2012b). External precision is based on the long-term reproducibility of an internal carbonate standard, processed regularly with each batch of samples, yielding $\pm 0.0.055\%$ for δ^{26} Mg and $\pm 0.04\%$ for $\delta^{44/40}$ Ca (1σ). Data are reported using the conventional delta notation relative to Modern seawater (for $\delta^{44/40}$ Ca) and the DSM-3 standard (for δ^{26} Mg).

RESULTS

All data used in this paper are included in Appendix S1.

Bulk samples

Mineralogy

In Unda, the dolomites contain between 43 mol% and 46 mol% $MgCO_3$, while in San Salvador the dolomites range between 42 mol% and 50 mol% $MgCO_3$. The samples show well-defined 101, 015 and 021 ordering peaks. Example scans are

presented in Appendix S1. In Clino the dolomites also show ordering peaks, but these are obscured by the presence of calcite (see later *Discussion*).

Clumped isotopes

The bulk Clino samples have Δ_{47} values (uncorrected for reaction at 90°C) ranging from 0.531 to 0.632%, translating to formation temperatures of 15 to 52°C using the modified calibration of Staudigel et al. (2018). The calculated temperatures tend to increase downcore from 25 to 340 m before they begin to oscillate throughout the remainder of the core, loosely correlating $(R^2 = 0.36)$ with the abundance of dolomite in the bulk carbonate (Fig. 4). The δ^{13} C values range from -0.73 to +5.32%, with the shallowest section of the core having the most negative values, increasing with depth to the most positive values around 323 m, then becoming more uniform at ca +3% through the rest of the core. The samples with the more positive δ^{13} C values also have some of the highest bulk aragonite percentages of any of the samples measured, although this correlation is not consistently present. The δ^{18} O values of the core range from -3.60 to +3.38%, with the most negative values at the top of the core and increasing to positive values over the next 160 m. Below 160 m, the δ^{18} O values vary between ca 0% and + 2.71% through the rest of the core.

Carbonate associated sulphate

San Salvador and Unda. In the San Salvador and Unda cores, there is little variability in the δ^{34} S values (+22.6, $1\sigma = 1.0\%$, n = 24 and +22.8, $1\sigma = 0.4\%$, n = 12, $\pm 1\sigma$) over the measured intervals (Fig. 5) and the values are similar to Plio-Pleistocene seawater δ^{34} S values (Burdett *et al.*, 1989; Paytan *et al.*, 2004; Bottrell & Newton, 2006).

Clino. Carbonates between ca 200 m and the first marine hardground at 367.04 mbmp show seawater-like δ^{34} S values. However, carbonates located between the first and second hardgrounds (367.04 mbmp and 492.55 mbmp) yield variable and much higher δ^{34} S values. Higher δ^{34} S values are also found below the second hardground. Both hardgrounds are associated with marked increases in dolomite abundance measured by XRD and changes to a higher bulk δ^{18} O value.

Calcium and magnesium isotopes

Clino. The δ^{26} Mg values range from -1.00 to -3.17‰ (1 σ = 0.31, n = 52) and $\delta^{44/40}$ Ca values between -0.63‰ and -1.43‰ (1 σ = 0.2, n = 51)

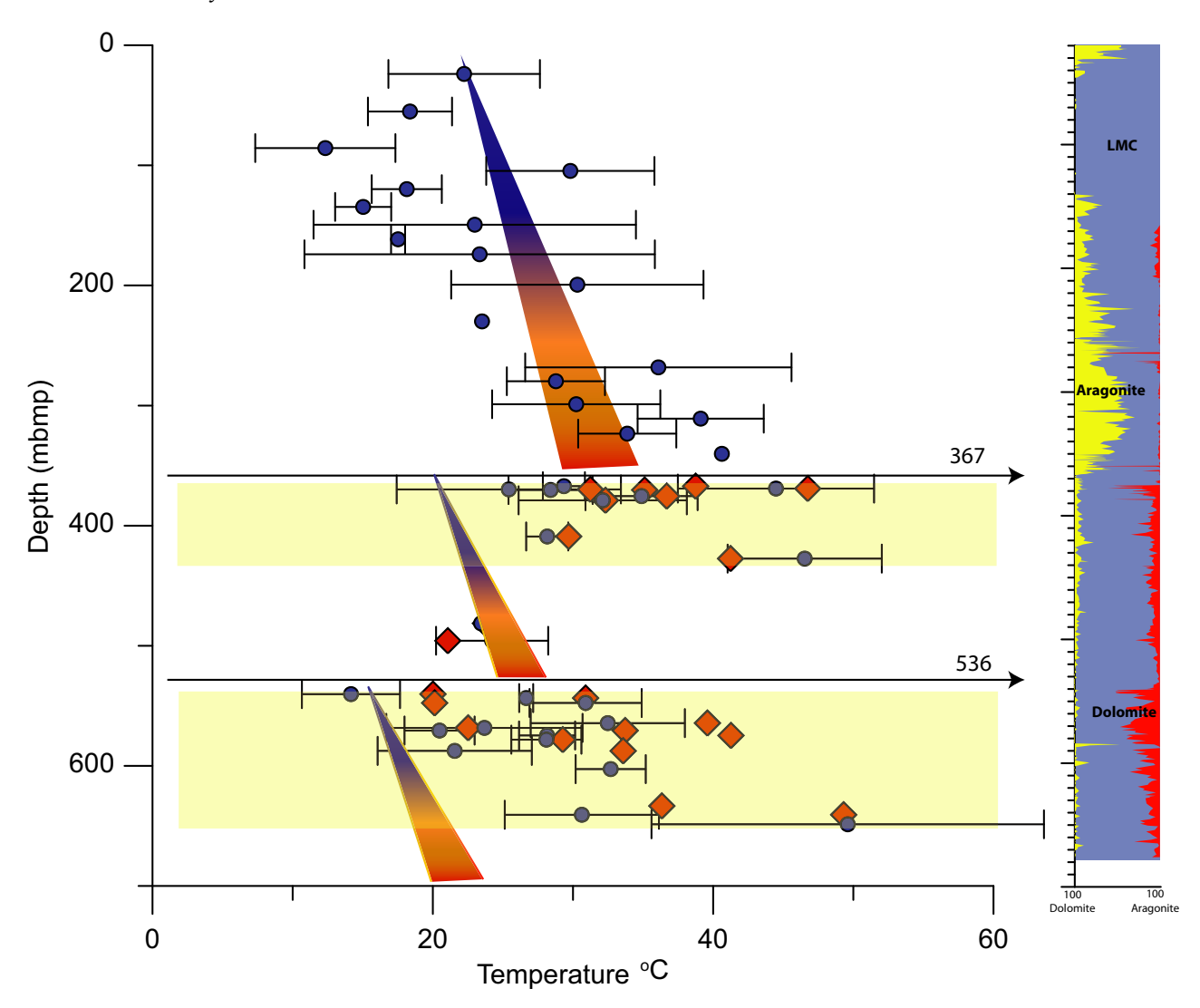


Fig. 4. Clumped isotope derived temperatures from bulk samples as a function of depth for bulk (blue dots) and separated dolomites (purple diamonds). Error bars represent ± 1 standard deviation of replicate analyses. The error bars have been omitted for the purposes of clarity from the dolomites. The two principal non-depositional surfaces at 367 metres below the mud pit datum (mbmp) and 536 mbmp coincide with the increase in the amount of dolomite. The hypothetical increase in temperature arising from the geothermal gradient is shown by the coloured triangle. The temperature of the bottom sediments is based on the estimated water depth of the hardground and the present water temperature at that depth (Staudigel & Swart, 2019). Temperatures appear to be close to those expected in the upper portion of the core (<367 mbmp). However, below 367 mbmp the bulk temperatures and the separated dolomites are elevated (yellow boxes).

(Figs 6 and 7). The downcore changes in bulk rock $\delta^{44/40}$ Ca and δ^{26} Mg values exhibit broadly antithetical patterns. This finding characterizes sediment discontinuity surfaces as well, where bulk rock transitions to higher $\delta^{44/40}$ Ca values and lower δ^{26} Mg values. There are also baseline shifts at 367 m due to changes in carbonate mineralogy, mostly in aragonite abundance. The mineralogical effect is best seen in the lithified sediment above 367 m where two large

oscillations in the $\delta^{44/40} Ca$ and $\delta^{26} Mg$ values correlate with changing aragonite abundance, but in opposite directions. It is noted, however, that the highest $\delta^{44/40} Ca$ value of –1.09‰ at 261 m is higher than the pelagic calcite end-member (–1.3‰), indicating that diagenesis affects the downcore patterns in $\delta^{44/40} Ca$ and $\delta^{26} Mg$ values as well

The pattern of intermittently high $\delta^{44/40}$ Ca and low δ^{26} Mg values associated with sediment

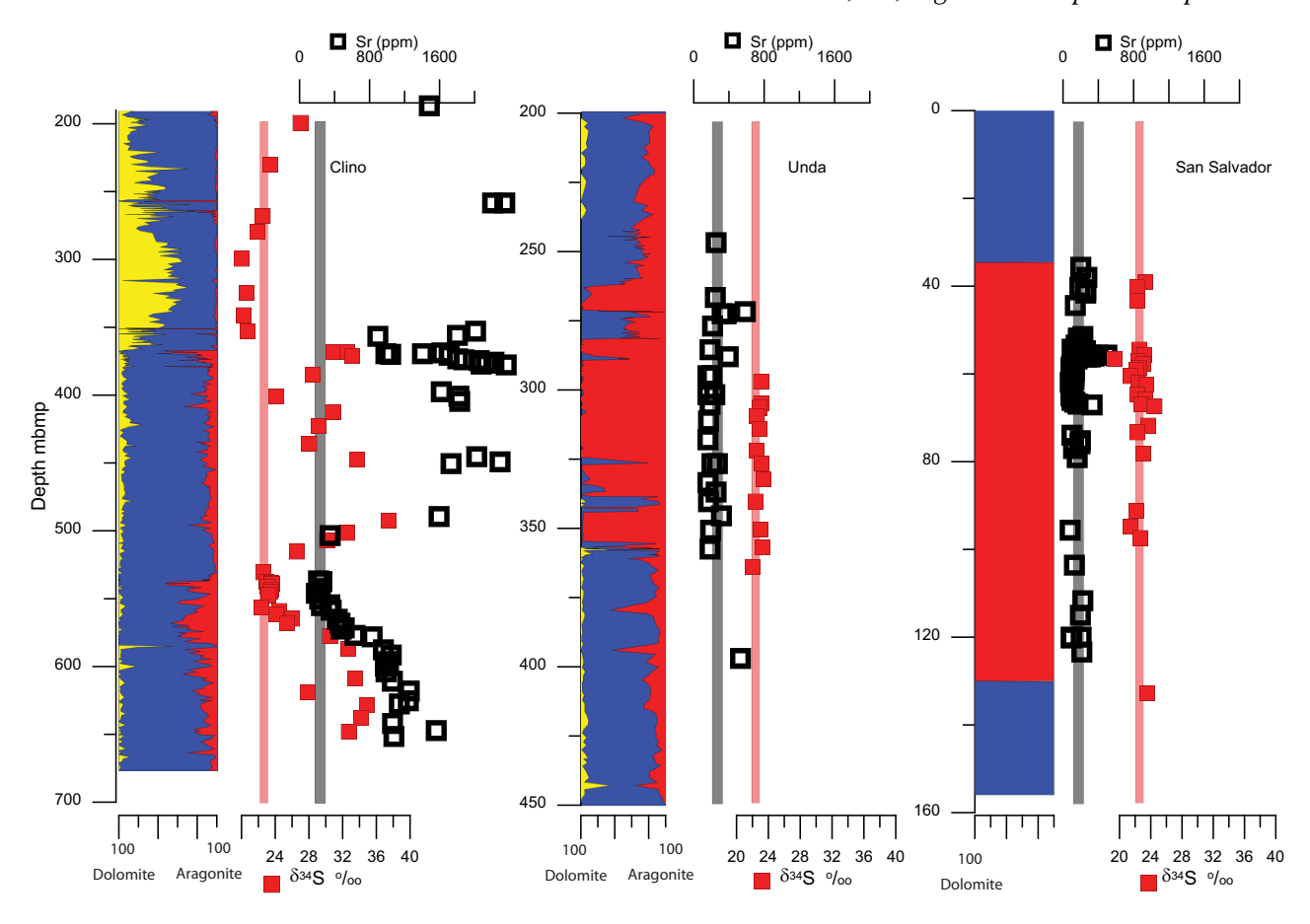


Fig. 5. Changes in the concentration of Sr concentrations (open black squares) and δ^{34} S values (red squares) as a function of depth from the Clino, Unda and San Salvador cores; Sr data for Clino and Unda are from Swart & Melim (2000) and for San Salvador from Dawans & Swart (1988). The red bar indicates the approximate δ^{34} S value of seawater during the Pleistocene–Late Miocene. The black bar represents the approximate Sr concentration in dolomite formed from normal seawater.

discontinuity surfaces is repeated throughout the core and is independent of downcore changes in bulk carbonate mineralogy, because aragonite is less common below 367 m and background dolomite is more common. Prominent examples occur at ca 256 m (multiple marine hardgrounds), 367 m (marine hardground and erosion), 379 m, 424 m and 474 m (reduced sedimentation rate), 536 m (marine hardground) and 542 m (reduced sedimentation rate) (Fig. 6). The major marine hardground and erosion surface corresponds to a change in depositional setting from lower to upper slope, i.e. an initial sea level low stand (with hardground development) followed by sea-level rise and increased imports of aragonitic sediment from the submerged platform. The stratigraphic interval below 367 m is another sea-level influenced

depositional sequence with a base at the 542 m hardground interpreted to reflect a hiatus in sedimentation, followed by increased sedimentation during the subsequent sea-level rise (Ginsburg, 2001), only this time it appears that less aragonite was imported from the platform based on the lower abundance of aragonite, higher abundances of planktonic foraminifera (2 to 10%) and baseline shifts to higher $\delta^{44/40}\text{Ca}$ and lower $\delta^{26}\text{Mg}$ values, which is consistent with higher pelagic contributions of primary LMC below 367 m.

The Mg/Ca ratio of dolomite separates in the Clino core is 0.65 ($1\sigma = 0.09$, n = 13) and 0.87 ($1\sigma = 0.2$, n = 43) for the massive dolomite in the San Salvador and Unda cores. The dolomite in both locations is Ca-rich. The XRD analysis shows that the Clino dolomite separates are on average $98 \pm 2\%$ pure dolomite. If only the five

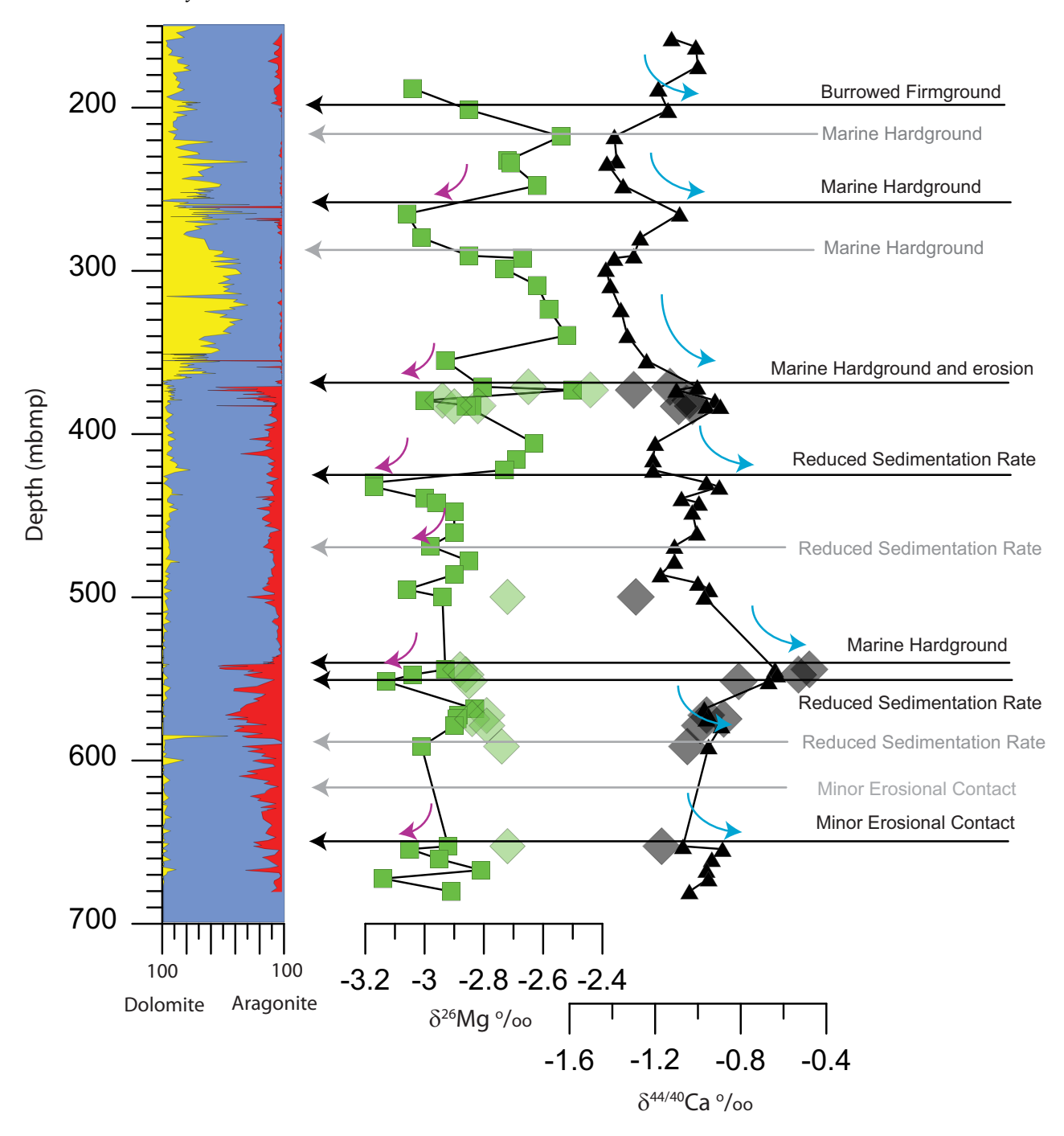


Fig. 6. Comparison of $\delta^{44/40}$ Ca and δ^{26} Mg values relative to non-depositional surfaces [data from Higgins et~al. (2018)]. Generally, the $\delta^{44/40}$ Ca values increase while the δ^{26} Mg values decrease associated with non-depositional surfaces. Pure dolomites isolated using a leaching method are shown in the larger faded green and grey diamond symbols. The surfaces identified by Kenter et~al. (2001) are marked, and in cases where they do not correspond to a surface the line and text are shown in grey. External precision as defined in the text is ca~0.08% for δ^{26} Mg and ca~0.06% for $\delta^{44/40}$ Ca, equal to or smaller than the size of the symbols.

samples that are 100% dolomite are considered, the average Mg/Ca ratio of the dolomites increases slightly to 0.73 ($1\sigma = 0.02$, n = 5).

San Salvador and Unda. San Salvador and Unda have a rather restricted range of $\delta^{26}Mg$ values: $\delta^{26}Mg_{San}$ Salvador = -2.79% (1 σ = 0.04%,

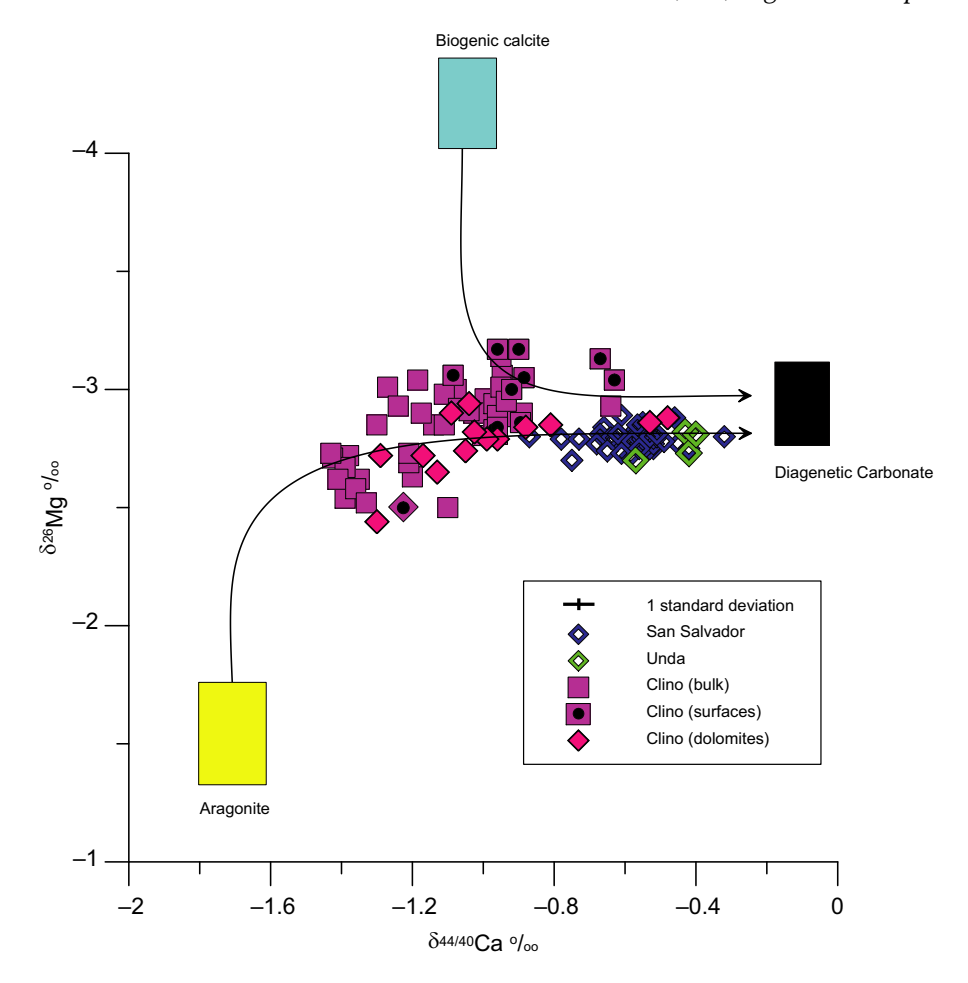


Fig. 7. Correlation between $\delta^{44/40}$ Ca and δ^{26} Mg values for samples from Unda, San Salvador and Clino; data from Unda and Clino are from Higgins *et al.* (2018). More positive $\delta^{44/40}$ Ca values and more negative δ^{26} Mg values are associated with non-depositional surfaces and open system diagenesis. Symbols with the black dots are those associated with non-depositional surfaces as shown in Fig. 6. Lines show pathways of diagenesis using model of Ahm *et al.* (2018). External precision as defined in the text is ca 0.08% for δ^{26} Mg and ca 0.06% for $\delta^{44/40}$ Ca, equal to or smaller than the size of the symbols.

n=39); $δ^{26}{\rm Mg_{Unda}}=-2.77$ ($1\sigma=0.06\%$, n=4). In contrast there is a slightly broader range of $δ^{44/40}{\rm Ca}$ values: $δ^{44/40}{\rm Ca_{San}}$ $_{\rm Salvador}=-0.65\%$ ($1\sigma=0.20\%$, n=61); $δ^{44/40}{\rm Ca_{Unda}}=-0.46\%$ ($1\sigma=0.08\%$, n=4).

Dolomite and calcite separates

For the calculation of the average values and other statistics, samples with >80% dolomite after acid treatments have been considered to be 'dolomite'.

Mineralogy

The percentage of dolomite in the Clino core varies from <1% to >50% (Swart & Melim, 2000). The scans of the non-purified material showed a range of peaks associated with both

minerals. The calcite peaks disappeared in the purified material showing ordering peaks at 101, 015 and 021. The intensity of the 015 peaks was reduced relative to the 110 peak indicating that the dolomites were disordered. Nevertheless, these dolomites are consistent with the definition of the mineral presented by Land (1980). Example scans are presented in Appendix S1.

Oxygen, carbon and Δ_{47} values. The disseminated background dolomites have $\delta^{13}C$ and $\delta^{18}O$ values that are respectively 1.20% to 1.90% more positive on average than their calcite counterparts based on a linear mixing model analysis. These are consistent with data from Swart & Melim (2000) (Fig. 8) with the exception of several $\delta^{18}O$ values estimated for LMC which fall below the

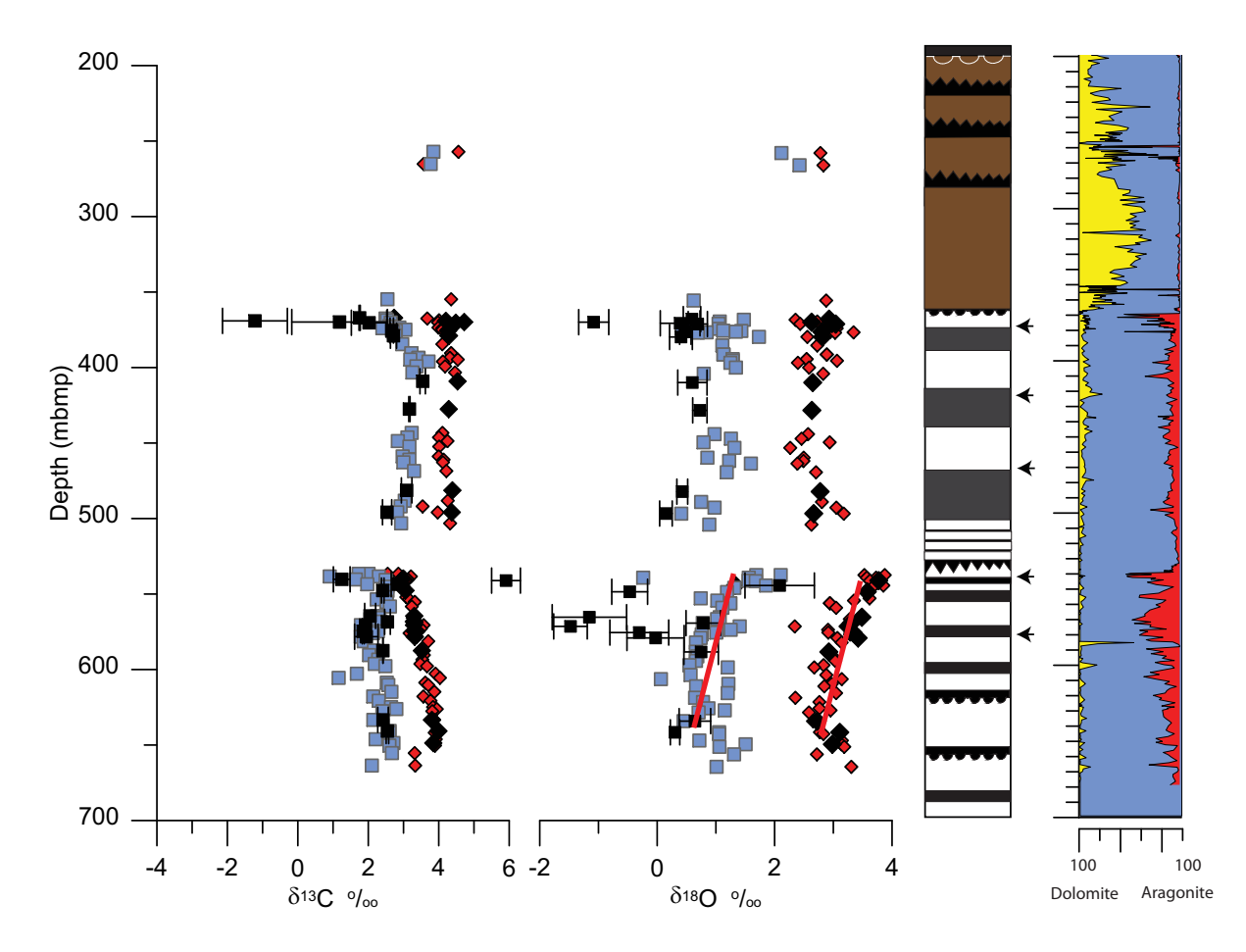


Fig. 8. Comparison of bulk $\delta^{13}C$ and $\delta^{18}O$ values of dolomite separates (black diamonds) and calculated value for the limestone (black squares). Data from Swart & Melim (2000) are shown in blue squares for bulk samples and red diamonds for dolomite separates Error bars representing $\pm 1~\sigma$ of the intercept are shown for the data from this study. The red line superimposed on the $\delta^{18}O$ values indicate the approximate gradient expected if the changes in $\delta^{18}O$ values were the result of temperature. Other errors are given in the Appendix S1.

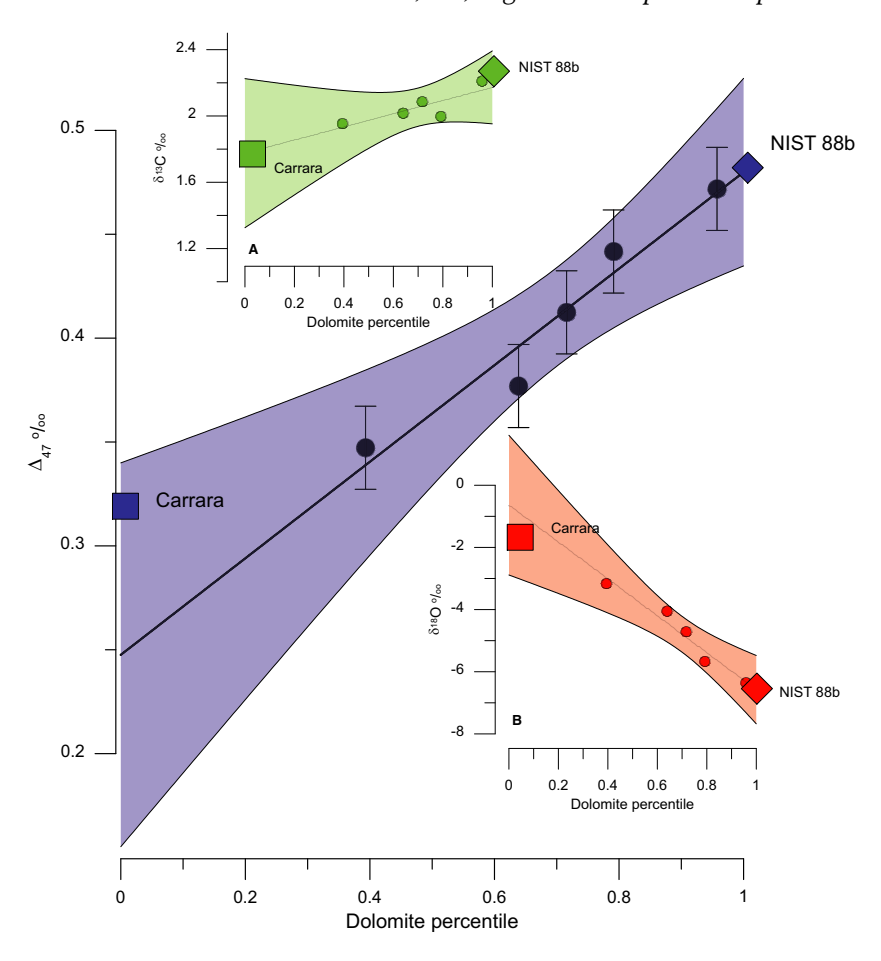
trend. These low values are a result of the error associated with the extrapolation from samples with high amounts of dolomite. With respect to the Δ_{47} values, the difference between the calcite and dolomite end members is not statistically significant with the exception of samples from 547.66 mbmp and 574.67 mbmp where the calcite end member is more negative than the dolomite by 0.061‰ and 0.058‰, respectively (Fig. 4).

Strontium. Pure dolomite end members from the Clino and Unda cores were measured for their Sr concentration by Swart & Melim (2000) and for San Salvador by Swart *et al.* (1987). The concentration of Sr in the Clino core ranges from 70 to 2378 ppm (Fig. 5). The lowest values occur

immediately below the 536 mbmp hardground surface. In comparison, dolomites from San Salvador and Unda had consistently lower Sr concentrations (generally less than *ca* 200 ppm).

Magnesium and calcium isotopes. The range in δ^{26} Mg values of the dolomite separates (0.5‰, n=13) is rather narrow considering the large variation in δ^{34} S values and Sr concentrations (Fig. 5). In fact, average δ^{26} Mg value of the background dolomite in the Clino core (-2.74 ± 0.14‰, n=8) is nearly indistinguishable from the massive dolomite found in the San Salvador (-2.79 ± 0.04‰, n=39) and Unda (-2.64 ± 0.05‰, n=4) cores, which yield a combined average δ^{26} Mg value of -2.77, $1\sigma=0.08$ ‰ (1σ ,

Fig. 9. Example of Δ_{47} values analyzed on samples in which quantities of our internal Carrara (calcite) laboratory standard and the NIST 88b standard (dolomite) were mixed to give a sample with 40% dolomite and then separated using the procedure of Swart & Melim (2000). The black circles show the individual analyses, the blue diamond the value for NIST 88b and the blue square the value for Carrara measured on pure samples. Values provided are for reaction at 90°C are uncorrected for any acid fractionation factor. Values for NIST 88b are within error identical to those measured by Defliese et al. (2015) at 90°C. The inserts show similar analyses of the $\delta^{13}C$ and δ^{18} O values. Pure samples are shown with the larger symbols. The δ¹⁸O values have been corrected using an acid fractionation factor of 1.008 (Sharma & Clayton, 1965), adjusted for the percentage of dolomite in the sample. The shaded areas represent 99% confidence limits.



n=51). The mean $\delta^{44/40}$ Ca values of the background dolomite in the Clino core is -1.08, $1\sigma=0.16\%$ (1σ , n=10). The mean $\delta^{44/40}$ Ca value of the massive dolomite in the San Salvador and Unda cores is -0.64, $1\sigma=0.22\%$ (1σ , n=61).

Separation of the standard calcite and dolomite material

Standards. The result of the separation of a synthetic mix of pure calcite and dolomite end members, uncorrected for acid fractionation, are shown in Fig. 9. These data show that the method accurately reproduces the Δ_{47} values of the end members within the 99% confidence limits of the extrapolation. The method also reproduces the $\delta^{13}C$ and $\delta^{18}O$ values of the original minerals. In the example a 40 : 60 mixture of dolomite and calcite was used. While it is possible to enrich the mixture close to 100% dolomite, it is not possible to enrich the calcite component. Hence the error on the extrapolation to 100% LMC is higher than extrapolation to 100% dolomite.

Clino. The $\delta^{13}C$ and $\delta^{18}O$ values have been calculated for the LMC end members in mixtures of calcite and dolomite using the intercept of the regression between percentage dolomite and the $\delta^{13}C$ and $\delta^{18}O$ values. These values are shown in Fig. 8 together with values calculated in the same manner by Swart & Melim (2000). The $\delta^{13}C$ values of the calcites are approximately 1‰ lower than the dolomites, while the calcite $\delta^{18}O$ values are approximately 3‰ lower than the dolomites.

DISCUSSION

Because glacioeustatic sea-level changes during the Pleistocene did not exceed *ca* 130 m (Lisiecki & Raymo, 2005), meteoric waters never penetrated deeper than *ca* 200 m. Therefore below *ca* 200 m the Clino core has only been affected by diagenesis within fluids derived from seawater (Swart & Oehlert, 2019). Nevertheless, the intensity of diagenesis throughout the portion of the core affected by only marine

derived fluids has been variable as a result changes in sedimentation rate, changes in original carbonate mineralogy and the presence of several major and numerous minor breaks in deposition (Fig. 2). Two major breaks in deposition occur, one at 367 mbmp where an unknown amount of sediment has been removed and one at 536 mbmp. The importance of these breaks is that they represent significant time gaps which can be ascertained using biostratigraphy (McNeill et al., 2001): ca 1 Myr for the 367 mbmp surface and 2 to 5 Myr for the 536 mbmp surface. Minor breaks in deposition, interpreted on the basis of sedimentology, occur at 197.4, 219.7, 256.0, 280.1, 379.0, 424.0, 474.0, 542.0, 585.1, 625.7 and 661.0 mbmp (Kenter et al., 2001), although the evidence for some of these is weaker than for others. For example, the surfaces at 379.0, 424.0, 474.0, 542.0 and 585.1 mbmp are inferred as a result of reduced sedimentation rate, an interpretation based on changes in the type of sediment.

Clumped isotopes

The Δ_{47} values of the bulk samples from Clino, including the upper portion affected by meteoric diagenesis, show a gradual decrease corresponding to temperatures of ca 23°C at the top of the section to 30°C at 200 mbmp (Fig. 4). This increase roughly corresponds to the rise in temperature expected as a result of the geothermal gradient, the magnitude of which in the Bahamas is well-characterized (Eberli et al., 1997a). Superimposed on this gradual decrease in Δ_{47} values (increasing temperature) is a considerable amount of variability that is significantly greater than the errors obtained on homogenous carbonates. The variability reflects the fact that bulk materials were analyzed and the samples within this interval are heterogeneous, being composed of different allochems. In particular, two aspects contributing to this variability are variations in the sediment composition and the precipitation of cements out of equilibrium. In the case of variations in the composition of the sediments, it has been reasonably well-established that certain types of carbonates such as scleractinian corals and echinoderms form their skeletons out of equilibrium with respect to Δ_{47} values (Saenger et al., 2012; Davies & John, 2018). Therefore, the decrease in Δ_{47} values between 70 mbmp and 120 mbmp, which corresponds to a coralrich interval (Manfrino & Ginsburg, 2001), can be explained by this mechanism. In addition, the phenomenon noted by Defliese & Lohmann

(2016) may result in meteoric cement precipitated within the vadose zone (above 100 to 120 mbmp) having Δ_{47} values out of equilibrium vielding warmer temperatures. Below 200 mbmp, within the zone of marine diagenesis, the clumped isotope derived temperatures from the bulk rock samples can be separated into three zones based on their downcore behaviour. Between 200 mbmp and the 367 mbmp erosional surface, the temperatures adhere closely to the proposed geothermal gradient, albeit with some variations as discussed above. At the time the erosional surface formed, the water depth was probably in excess of 100 to 200 m. suggesting an ambient temperature between 15°C and 20°C. While the dolomite forming immediately beneath the surface would have formed at these temperatures, the Δ_{47} derived temperatures are significantly higher (30 to 50°C). A similar phenomenon occurs below the lower hardground at 536 mbmp, but not until 40 to 50 m below the surface. Close to this hardground Δ_{47} values yield temperatures close to those expected (ca 15 to 20°C). While the precise explanation for the warmer temperatures at 40 to 50 m below the 536 mbmp hardground are unknown, the most probable cause is that high alkalinity, related to BSR, created non-equilibrium conditions with regard to the clumped isotope proxy leading to depressed Δ_{47} values. Similar non-equilibrium behaviour has been observed associated with methane seeps where the gas is anaerobically oxidized by SO_4^{2-} thereby increasing alkalinity and consequently precipitating high levels of carbonate (Loyd et al., 2016). These workers postulated that kinetic effects resulting from CO2 hydration and hydroxylation (and dehydration and dehydroxylation) reactions induced anomalous clumped isotope temperatures. Additional factors proposed by Loyd et al. (2016) to explain non-equilibrium phenomena in the Δ_{47} values were speciation effects associated with dissolved inorganic carbon, mixing and rapid precipitation. Anomalous Δ_{47} values at the 367 mbmp disconformity are attributed to the presence of an erosional surface (Kenter et al., 2001). Erosion removed an unknown amount of sediment truncating the section and removing the portion subject to early diagenesis.

Calcium isotopes

The bulk $\delta^{44/40}$ Ca values are controlled by both changes in primary mineralogy and syndepositional and

early marine diagenesis. The mineralogical control is best observed above 367 mbmp where downcore changes in aragonite abundance relative to calcite causes two large oscillations in the bulk $\delta^{44/40}$ Ca values. If all of the aragonite in this part of the core were to eventually invert to calcite in a closed system, the downcore variation in $\delta^{44/40}$ Ca would be preserved in the diagenetically stabilized LMC, as there is no fractionation of Ca isotopes at the low precipitation rates associated with diagenetic recrystallization of carbonates (Fantle & DePaolo, 2007; Jacobson & Holmden, 2008). Accordingly, sedimentary carbonate successions recording large variations in sedimentary $\delta^{44/40}$ Ca values in the deep geological past where aragonite has long ago inverted to calcite must be evaluated for the effects of mineralogy (aragonite versus calcite) and the style of early marine diagenesis (Husson et al., 2015; Kimmig & Holmden, 2017; Higgins et al., 2018). Facies-dependent changes in carbonate precipitation rate occurring independently of changing carbonate mineralogy may also need to be considered (Farkas et al., 2007; Holmden et al., 2012a).

The diagenetic framework for interpreting $\delta^{44/40}$ Ca values in carbonates proposed by Higgins et al. (2018) and modelled by Ahm et al. (2018) is based on the premise that if diagenesis occurs in an open system where the sedimentary pore fluids are continually replenished by seawater, then recrystallized carbonates will be altered towards higher $\delta^{44/40}$ Ca values compared to the original carbonates. The reason is that seawater is 44Ca-enriched relative to all inorganically and biologically precipitated marine carbonate polymorphs in the surface ocean, including HMC, aragonite and LMC, because precipitation rates in seawater are high enough to induce per mil level kinetic isotope effects favouring ⁴⁴Ca depletion in the produced carbonates. At the very low precipitation rates characterizing diagenetic systems, carbonate precipitation occurs without fractionation under conditions approaching chemical and isotopic equilibrium (Fantle & DePaolo, 2007; Jacobson & Holmden, 2008). Thus, the bulk carbonate sediment will become isotopically more positive if seawater derived Ca is present in the pore fluids when the primary carbonate minerals recrystallize to diagenetic LMC and dolomite, such as occurred during hardground formation in the Clino core. Two notable examples are 540.288 mbmp hardgrounds at 543.555 mbmp that gave much higher $\delta^{44/40}$ Ca

values of -0.48% and -0.53%, respectively. The cumulative volumes of fluid (relative to sediment) advected through the flushed zone when these two hardgrounds formed is comparable to the cumulative fluid-rock ratios forming massive dolomites in the San Salvador and Unda cores based on their comparable δ^{44/40}Ca average value -0.55, $1\sigma = 0.106\%$ (n = 51). Although these two hardgrounds are exceptional, other hardgrounds in the Clino core also yielded dolomite separates that are higher in $\delta^{44/40}$ Ca [averaging -1.08, $1\sigma = 0.16\%$ (n = 10)] than platform-sourced primary aragonite (-1.50%) and pelagic-sourced primary calcite (-1.30%), indicating diagenetic uptake of Ca from seawater during their formation. It follows that seawater must have also supplied reactive Mg for dolomite formation, consistent with seawater signatures exhibited by CAS δ³⁴S values in hardgrounds and massive dolomite. However, bulk δ^{44/40}Ca values at Clino are systematically lower than those at either San Salvador or Unda; a difference attributed to the dilution of seawater calcium in the dolomitizing fluid with isotopically more negative calcium from carbonate sediment dissolution in a more sediment-buffered diagenetic system (Ahm et al., 2018; Higgins et al., 2018). Isotopic studies of dissolved Ca in marine sediment pore fluids (Fantle & DePaolo, 2007; Turchyn & DePaolo, 2011; Higgins et al., 2018) show that dissolution of metastable carbonates is capable of rapidly resetting pore fluid $\delta^{44/40}$ Ca values. For example, Ca from seawater is totally mixed out of the pore fluids at Ocean Drilling Program (ODP) Site 1007 at 65 m depth below the sediment-water interface and at ODP Site 1003 by 86 m depth (Higgins et al., 2018).

This study shows that if the continuity of sediment deposition was frequently disturbed by hiatuses, then marine diagenesis involving Ca from seawater could lead to stratigraphic variation in 44Ca-enrichments in the bulk rock that could be mistakenly interpreted as evidence for the effects of global change on ocean Ca cycling, particularly in shallow epicratonic seas where the continuity of sedimentation is more likely to be disturbed by currents, waves, storms, burrowing animals and relative sea-level change. This diagenetic caution adds to previously recognized concerns regarding misinterpreting facies-dependent stratigraphic changes in carbonate polymorph mineralogy as genuine records of changing δ^{44} Ca of seawater in the geological past (Kimmig & Holmden, 2017; Ahm et al., 2018;

Higgins et al., 2018) and other local Ca cycling effects in epeiric seas, such as submarine groundwater discharge, which can lower the δ⁴⁴Ca of seawater in circulation restricted settings (Holmden et al., 2012a).

Magnesium isotopes

The behaviour of bulk δ^{26} Mg values in the Clino core is generally opposite to that of Ca isotopes. Using pore fluid geochemistry in deep sea carbonates as a natural laboratory for monitoring diagenetic reactions, two studies have inferred different but similarly low fractionation factors ($\cong 1000 \text{ ln}\alpha$) of -3.7% and -4.5% (Higgins & Schrag, 2012; Fantle & Higgins, 2014) for diagenetic LMC. These are larger than the fractionation factors measured for precipitation of biotic and abiotic aragonite and abiotic calcite (Saenger & Wang, 2014). Only biotic calcite typically reaches values this low. Importantly, the equilibrium isotope fractionation factor for diagenetic LMC is nearly twice as large as the fractionation factor associated with high Mg-calcite (HMC) and aragonite (Saenger & Wang, 2014) and when these metastable minerals are transformed into LMC during marine diagenesis in an open system the bulk values is altered towards lower δ^{26} Mg values. The effect will not be observed, however, if only a small amount of LMC is produced in static pore fluids. Therefore, to create large effects like those associated with sediment hardground surfaces in the Clino core, a more open diagenetic system is needed to refresh sedimentary pore fluid Mg during diagenetic calcite formation. On the other hand, if dolomite is also formed during marine diagenesis, then the bulk $\delta^{26}Mg$ values will be altered to higher values, approaching the limit of -2.74 ($1\sigma = 0.14\%$, n = 8), which is the δ²⁶Mg value of dolomite in the Clino core based on analyses of dolomite separates, the same value that characterizes dolomite in the San Salvador and Unda cores, -2.78 ($1\sigma = 0.06\%$, n = 43). Therefore, whether it is background dolomite in Clino or more pervasively dolomitized carbonate in San Salvador and Unda (Higgins et al., 2018), dolomite formed under both relatively closed and open diagenetic conditions appears to give similar δ^{26} Mg values in the Bahamas.

Before discussing the significance of this finding it is important to note that, in any marine rocks containing dolomite, mass balance considerations dictate that the δ^{26} Mg value of bulk sediment has a strong tendency to be controlled by the δ^{26} Mg value of dolomite, because this mineral contains the highest abundance of Mg of any of the common carbonate polymorphs. For example, Kimmig & Holmden (2017) showed that a 2 to 3% positive change in bulk δ^{26} Mg values recorded in a succession of late Ordovician carbonates in Nevada could be attributed to just 12 mol% increase in background dolomite in the section. The δ^{26} Mg values for dolomite separates from the Clino core are plotted in Figs 6 and 7. As expected, there are number of stratigraphic levels in the core where δ^{26} Mg values of the bulk closely approach the δ^{26} Mg value of dolomite, thus indicating that background dolomite is the dominant Mg reservoir at these depths. In rocks with lower concentrations of dolomite, the bulk δ^{26} Mg values is altered to values of ca -3.1%, ca 0.3% lower than the average dolomite value of -2.77%. This implies that the Mg concentration of diagenetic LMC at these stratigraphic levels is relatively high with a δ^{26} Mg value close to -3.1% (Fig. 5), or relatively low concentration with a δ^{26} Mg value <<-3.1%. A process supporting the first explanation is the closed system conversion of HMC to LMC, where the δ^{26} Mg value of HMC is close to -3.1‰ (cf. Fantle & Higgins, 2014). The second explanation requires a more open diagenetic system to produce very low δ²⁶Mg values for diagenetic LMC. In summary, there are two factors to consider regarding whether marine diagenesis will drive bulk δ²⁶Mg values to higher or lower values: (i) the amount of ²⁶Mg-enriched dolomite or HMC; and (ii) the Mg concentration and isotopic composition of ²⁶Mg-depleted diagenetic LMC. The finding that many of the sedimentary hiatuses in the Clino core record shifts to lower bulk δ^{26} Mg values indicates that diagenetic LMC formed in addition to dolomite in the hardgrounds. While a closed system transformation of HMC to LMC could produce similar results, evidence from Sr concentrations and δ^{34} S values favour an open system with SO_4^{2-} and Sr²⁺ mass transfers between seawater and pore fluids during sedimentary hiatuses. Thus, it seems more likely that diagenetic LMC with very low δ^{26} Mg values is driving bulk rocks towards lower values in the hardgrounds.

Mass balance considerations can be used to gain additional insights into the reason for the strikingly similar δ²⁶Mg values between background and massive dolomite in the Bahamas and the insensitivity to diagenetic systems. To accomplish this aim, consider δ^{26} Mg values from ODP Site 1131 drilled on the Great Australian Bight (Higgins et al., 2018). The upper 70 m of this core is predominantly HMC and aragonite (25 to 70%) with small amounts of LMC (<20%), yielding an average bulk δ^{26} Mg value of -3.02 ($1\sigma = 0.06\%$, n = 12). Because there is very little Mg in aragonite, mass balance considerations dictate that the δ^{26} Mg value of HMC must be close to the bulk value. Below 70 m the dominant Mg bearing mineral is dolomite and the average bulk δ^{26} Mg values is $-3.00 (1\sigma = 0.13\%, n = 32)$, which is nearly the same value as HMC in the top 70 m. These observations suggest that HMC is transforming to dolomite during burial with no change in δ^{26} Mg values. However, the true average δ^{26} Mg value of dolomite and HMC at Site 1131 will be slightly higher than -3.0% as a result of contributions from Mg with more negative δ^{26} Mg values in the LMC fraction of the bulk sediment. This can be corrected for by examining the relationship between the δ^{26} Mg values and Ca/Mg ratios (Fig. 10). Despite the scatter in the distribution, the data are reasonably well-correlated with a R^2 of 0.44 when combined with the bulk Clino data and dolomite separates, suggesting a two-component mixture between dolomite with differing δ^{26} Mg values. The combined average Mg/Ca ratio for dolomite separates from Clino and massive dolomite from the Salvador and Unda cores is $1\sigma = 0.02\%$. Substituting this value for Mg/Ca ratio into the equation on the relationship shown in Fig. 10 yields an end-member δ^{26} Mg value of -2.79% for background dolomite that

is representative of both the Australian and Bahamas settings and which is nearly identical to the average value of -2.78, $1\sigma = 0.06\%$ for massive dolomite in the San Salvador and Unda cores and background dolomite in the Clino core. Bulk values from the HMC dominated upper part of the ODP Site 1131 also plots on or close to the average mixing line between dolomite and LMC, which is evidence that HMC has a similar δ^{26} Mg value as dolomite. Hence it apparently does not matter whether dolomite forms by 'inversion' of HMC in a closed diagenetic system, or by replacement of aragonite or LMC in open diagenetic system. As long as the temperature of the latter is close to ambient Earth surface temperatures, they will both end up with very similar δ^{26} Mg values.

Bacterial dolomites

There has been a considerable literature on the occurrence of dolomites that form as a result of the activities of bacteria, so-called bacterial dolomite (Vasconcelos & McKenzie, 1997; Warthmann et al., 2000). Such a model of formation might conceivably also be responsible for the background dolomite found in the majority of the Clino core, where the lithified sediments have elevated $\delta^{34}S$ values indicating bacterial sulphate reduction and Δ_{47} values suggestive of carbonate disequilibrium as a result of high alkalinity. In contrast, the dolomites found in Unda and San Salvador are formed in more open marine conditions as indicated by

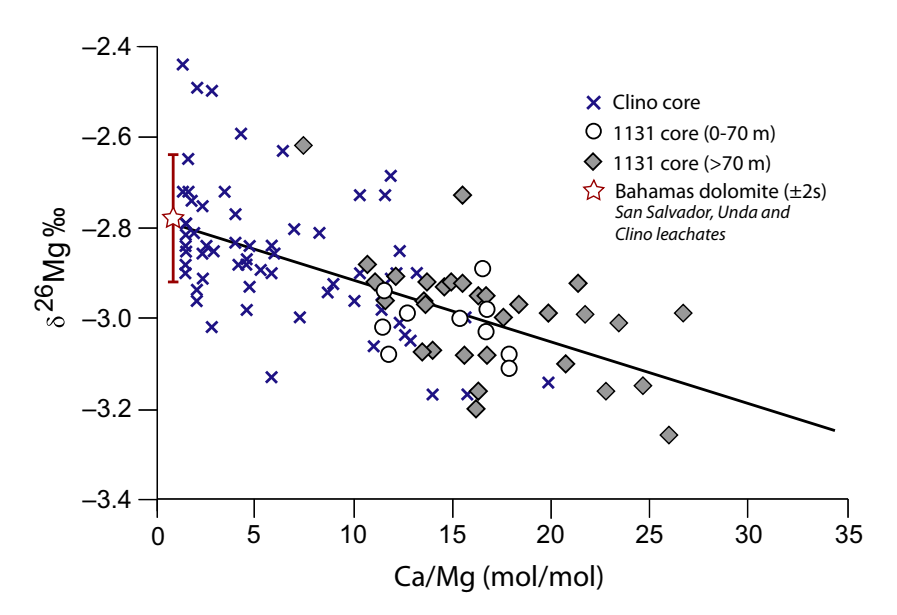


Fig. 10. Relationship between the Ca/Mg ratio and δ^{26} Mg values of samples from Ocean Drilling Program (ODP) Site 1131 (Higgins *et al.*, 2018) and dolomites from the Bahamas (this study).

^{© 2020} The Authors. Sedimentology © 2020 International Association of Sedimentologists, Sedimentology

their marine $\delta^{34}S$ values, relative low Sr concentrations, higher $\delta^{44/40}Ca$ and Δ_{47} values that suggest dolomitization by unaltered seawater. Considering that it has been suggested that bacterial dolomites might have distinct δ^{26} Mg values (Carder et al., 2005), it is therefore remarkable that there are such small differences in δ^{26} Mg values between background dolomites formed under 'closed' diagenetic conditions in the Clino core and massive dolomite formed under 'open' diagenetic conditions in Unda and San Salvador (Fig. 10). This either tends to discount the suggestion that δ^{26} Mg values can be used to identify bacterial dolomites, or that if such differences do exist that the formation of dolomites with sulphate reduction signatures in the Clino core, while possibly being mediated by bacterial activity, are not bacterial dolomites per se.

CHANGES IN CARBON, OXYGEN AND SULPHUR ISOTOPES

Changes in the δ^{34} S, δ^{18} O and δ^{13} C values of the carbonates within the zone of marine diagenesis can be described using a numerical model applied to the interval below the 536 m non-depositional surface. This surface represents a hiatus of between ca 2 to 4 Myr (McNeill et al., 2001) (Fig. 9) and during this time various chemical constituents, such as Ca^{2+} , Mg^{2+} , SO_4^{2-} and HCO_3^- , diffused into the sediments under the influence of concentration gradients generated by the formation of diagenetic minerals such as dolomite and calcite. Bacterial sulphate reduction creates carbonate alkalinity, which in turn raises the saturation index of dolomite, thus, favouring precipitation and leading to the concentration of dolomite, up to 52 wt%, which occurs approximately 50 to 100 cm below the surface (Fig. 2). Over the next 100 m the concentration gradually decreases to <10%. The mean concentration of dolomite in this interval is 20 wt% and ranges between 0 wt% and 52 wt%. As the concentration of dolomite reaches a maximum close to the hardground and then decreases with depth, it is likely that the Mg necessary for dolomite formation was supplied from the overlying seawater diffusing downward along a concentration gradient in Mg. The amount of Mg supplied during the hiatus can be calculated using a standard diffusion equation (Eq. 2). In this equation the flux (Flux) of a chemical constituent is a function of the

concentration gradient ($\delta c/\delta z$), the bulk diffusion coefficient (Db) and the time (t) and assuming that the concentration of Mg decreases to zero at a depth of 100 m below the hardground. This calculation indicates that sufficient Mg would be supplied over 5 Myr to dolomitize ca 10% of the sediment, using a Mg diffusion coefficient of 6×10^{-6} cm² s⁻¹ (Li & Gregory, 1974):

$$Flux = \delta c / \delta z * Db * t$$
 (2)

Although this calculation only supplies approximately 50% of the mean concentration of dolomite in this interval, the estimate is not unreasonable considering uncertainties in the bulk diffusion coefficient, the duration of the hiatus and the contribution of Mg from the dissolution of high-Mg calcite. In addition, there are several other surfaces within this interval that represent time gaps during which Mg can diffuse into the sediments from the overlying seawater and thereby contribute additional Mg. An advective source of Mg can be ruled out as a result of the diffusive type gradients in the concentration of Sr and δ^{18} O values of the dolomites (see later *Discussion*).

Strontium

The dolomites in the interval immediately below the 536 m hardground have Sr concentrations between 200 ppm and 300 ppm, close to what might be expected for open-system marine dolomite (Vahrenkamp & Swart, 1990). The interval, over which the concentration of Sr in dolomite is relatively invariant (Fig. 5), is similar to the zone observed in the cores drilled off the margin of Great Bahama Bank during ODP 166. The zone was designated the 'flushed zone' as it was proposed that active advection of seawater removed any geochemical and geothermal gradients (Eberli et al., 1997a; Kramer et al., 2000). Below this depth the concentrations of Sr in the dolomites gradually increase, similar to those observed at many Deep Sea Drilling Project (DSDP) and Ocean Drilling Program (ODP) sites (Gieskes et al., 1986; Kramer et al., 2000) in which the concentration of elements in the pore waters has been interpreted as being diffusively controlled. The maximum Sr concentration in bulk rock below the 536 mbmp hardground is 800 ppm, a value calculated by Swart & Melim (2000) to be in approximate equilibrium with celestine (SrSO₄) in porewaters (Baker, 1985; Baker & Bloomer, 1987). The flux of Sr^{2+} along such gradients can be modelled and the total amount of Sr removed estimated as a measure of the amount of recrystallization (Baker *et al.*, 1982). However, such estimates tend to underestimate the actual amount of recrystallization as no allowances are made for removal of Sr^{2+} as celestine (Guzikowski, 1987). The presence of the steep gradient in the concentration of Sr^{2+} precludes the possibility of large-scale fluid advection, a notion supported by the $\delta^{44/40}$ Ca values. The δ^{26} Mg data in contrast suggest a more open system throughout, clearly in conflict with the Sr concentrations and $\delta^{34}S$ values (Fig. 6).

Oxygen isotopes and clumped isotopes

The $\delta^{18}O$ values of the calcite and dolomite components are elevated just below the 536 m hardground with calcite having values close to +2% and dolomite +4% (Fig. 8). These values translate into temperatures of about 12 to 15°C for calcite and 16 to 18°C for dolomite associated with the hardground, assuming a δ^{18} O value for water of 0%. The $\delta^{18}O$ value of the calcite component of the rock decreases with increasing depth equivalent to a geothermal gradient of 16°C/1000 m (assuming a constant δ¹⁸O value of the fluid), while the δ^{18} O value of the dolomite decreases at a rate of 30°C/1000 m and is closer to the presumed geothermal gradient (Nagihara & Wang, 2000). The explanation for the difference can be modelled using an approach similar to that used by Lawrence et al. (1975). In this method, the sedimentary column, in this case the 100 m underlying the 536 m hardground, can be constructed using a series of 1 m thick units (boxes). Each box is allowed to recrystallize at a prescribed rate and the resultant δ^{18} O values of the fluids, diagenetic carbonate and bulk carbonate calculated and used as an input for the next box in the sediment column. During the dissolution and precipitation reactions it is assumed that the pore waters remain oversaturated to the minerals involved and that there are no kinetic effects. Products of the reactions within each box are allowed to diffuse along concentration gradients into the overlying and underlying boxes before the next box is deposited. Relevant diffusion coefficients have been taken from Li & Gregory (1974). The boundary conditions (initial δ^{18} O value of sediment, initial δ^{18} O value of fluid, molar water/rock ratio, rate of recrystallization, geothermal gradient and bottom water temperature) are listed in Table 2. Once the sedimentary column has been constructed, the δ^{18} O values of the fluid, the newly formed diagenetic carbonate and the bulk carbonate can be calculated as a function of depth and the model output compared to the actual data. In this case it can be assumed that dolomite represents the diagenetic carbonate, whilst the bulk carbonate represents a composite of the diagenetic low-Mg calcite and the original sedimentary carbonate. The results (Fig. 11A) indicate that the temperatures, calculated from the δ^{18} O values of the calcitic components, decrease less than expected from the geothermal gradients. In contrast, temperatures calculated using the δ¹⁸O values of the dolomite show a steeper gradient and are close to the actual geothermal gradient as measured in sediments on the margin of

Table 2. Parameters used in modelling (Fig. 11).

Parameter	Values	Reference
Initial δ^{18} O value of sediment	+1‰	Swart <i>et al.</i> (2009)
Initial δ^{18} O value of fluid	0.3‰	Swart (2000)
Molar water/rock ratio	1.0	This paper
Geothermal gradient	$35^{\circ}\text{C km}^{-1}$	Nagihara & Wang (2000)
Bottom water temperature	12°C	Nagihara & Wang (2000)
Rate of recrystallization	$0.25\%\ m^{-1}$	This paper
Rate of BSR	$0.6m\text{m}m^{-1}$	This paper
SO_4^{2-} H ₂ S fractionation	1.072	Wortmann et al. (2001)
Concentration of SO_4^{2-} in carbonate	2000 ppm	Gill et al. (2008)
Partition coefficient of S (K_S) into diagenetic carbonate	0.0005	This paper

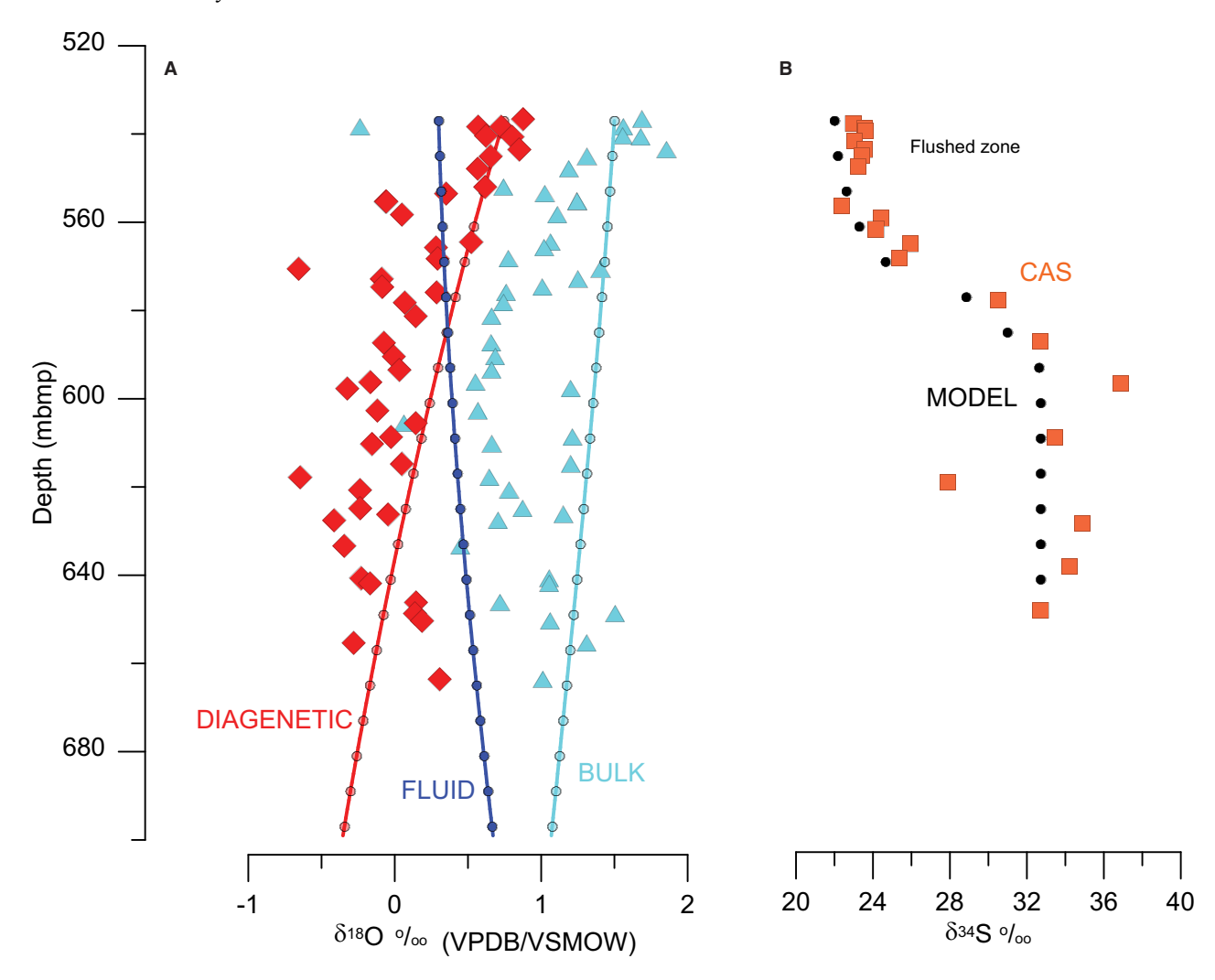


Fig. 11. (A) Output of modelling of δ^{18} O values for diagenetic component, bulk and fluid (lines with smaller solid circles). The actual data for the diagenetic component (red diamonds) and bulk components (blue diamonds). The values for dolomite have been adjusted for the fractionation between calcite and dolomite and show a steeper downcore trend than the calcite. (B) Output for the modelling of the δ^{34} S values (red circles) compared to measured data (red squares). Complete bacterial sulphate reduction (BSR) is assumed by a depth of 50 m below the 537 mbmp hardground.

Great Bahama Bank by Nagihara & Wang (2000). The discrepancy between the two results reflects the fact that the calcitic component represents mixtures of original and diagenetic carbonate, while the dolomite reflects only the diagenetic carbonate. It should also be noted that the more recent equation linking dolomite to temperature (Horita, 2014) yields temperatures in excess of those expected for this proposed water depth. Although the magnitude of the decrease in δ^{18} O values in the dolomites is similar to that expected for recrystallization along the expected geothermal gradient, no

account was made for the increase in the $\delta^{18}O$ values of the pore fluids as would be expected during the recrystallization of such sediments in the presence of an increase in temperature. Ideally, this could be corrected for by using the clumped isotope proxy, but in the case of this study, the high amounts of BSR apparently produce higher than expected temperatures using the clumped isotope proxy, precluding its use in this situation. In addition, the model predicted only a small change in the $\delta^{18}O_{fluid}$ value over this interval, therefore validating the assumptions made.

Sulphur isotopes

The δ^{34} S values of CAS have been widely used both as an indicator of the δ^{34} S values of oceanic SO₄²⁻ (Strauss, 1997; Kampschulte & Strauss, 2004; Lyons et al., 2005) as well as to understand diagenetic processes (Marenco et al., 2008; Lovd et al., 2012; Rennie & Turchyn, 2014; Present et al., 2015; Present et al., 2019). The primary control of the $\delta^{34}S$ values of the oceans relates to the weathering of sulphide deposits which returns S with a lower δ^{34} S value to the oceans and the processes of BSR which enrich the residual SO_4^{2-} pool in $^{34}S.$ As regards the Clino core, the region below the 536 m hardground in Clino shows an increase in $\delta^{34}S$ values of the CAS which closely parallels the changes in the concentration of Sr within the dolomite (Fig. 5). As the δ^{34} S values were measured in the bulk carbonate, not the dolomite, they reflect mixtures of original carbonate, with normal δ³⁴S values and diagenetic calcite enriched in 34S arising from BSR. The change in the δ³⁴S can be modelled by adding a module to the carbonate recrystallization model which decreases the concentration of SO_4^{2-} resulting from BSR concomitant with the recrystallization of carbonate. As the carbonate dissolves and reprecipitates, the CAS is released into the pore space and becomes available for BSR utilizing the in situ organic material or biogenic gas produced lower in the section. A smaller amount of SO_4^{2-} with the $\delta^{34}S$ value of the pore fluid is then incorporated into the newly precipitated carbonate. The extra variables which need to be considered are the concentration of S in the original carbonate material, the rate of BSR relative to carbonate recrystallization, the fractionation of ³⁴S during BSR as a function of temperature and the partition coefficient of S into the newly formed carbonate (Table 2). The partition coefficient (K_S) for the incorporation of the SO_4^{2-} into the carbonate is estimated relative to calcium and is calculated based on the mean S/Ca in calcite of ca 1 mmol mol⁻¹ (van Dijk et al., 2019). While there is probably a great deal of uncertainty in the value of Ks, its precise value will affect the magnitude of the increase in the δ^{34} S value of the porewater, with higher values leading to a greater increase. In this particular case, it is assumed that BSR is complete at a depth of 50 m below the hardground while carbonate recrystallization continues throughout the sequence reaching 50% at 100 m below the hardground. Using these

parameters, the observed CAS values agree well with the modelled values (Fig. 11B). Note that a fractionation factor of 1.072 measured by Wortmann *et al.* (2001) was used because it reproduces the δ^{34} S value of +36% measured in the Clino samples, while with lower values ($\alpha = 1.046$) suggested by other workers (Kaplan & Rittenberg, 1964) produce lower CAS δ^{34} S of +30%.

In contrast to Clino, the $\delta^{34}S$ values of the CAS in both the San Salvador and Unda cores $(+22.6, 1\sigma = 1.0\%, n = 24 \text{ and } +22.8, 1\sigma = 0.4\%.$ n = 12) show little variation within the dolomitized intervals and are similar to Mio-Pliocene seawater δ³⁴S values measured using marine barite (Paytan et al., 1998) and records $\delta^{34}S_{CAS}$ values, and therefore suggests an open diagenetic system in which the sediments while they were in the process of being dolomitized were continually flushed by seawater, thus imparting a contemporary δ³⁴S value. While such findings are similar to those observed in ancient deposits such as the Permian Capitan reef complex, where original δ^{34} S values are preserved in carbonates altered in high-energy environments (Present et al., 2019), they are apparently at odds with studies which found preserved δ³⁴S_{CAS} values within sediments with low rates of deposition (Rennie & Turchyn, 2014). Such differences can be readily explained because, in the case of the sediments described by Rennie & Turchyn (2014), the organic content of the sediments had probably been reduced by oxidation at the sea floor; elevated $\delta^{34}S_{CAS}$ values will only be preserved when carbonates recrystallize in the presence of pore-water sulphate with an elevated δ^{34} S value due to contemporaneous BSR. If the sediments are diagenetically stabilized prior to or after the zone of elevated $\delta^{34}S$ values in the pore waters, the elevated δ^{34} S values will not be preserved in the CAS.

Carbon isotopes

The δ^{13} C values of the calcite components immediately below the 536 mbmp hardgrounds show a small, but significant, decrease (from +2‰ to ca 0‰). Based on the conclusion that advective transport of fluids was taking place in the upper ca 20 m, the decrease in δ^{13} C values was probably a result of recrystallization within bottom waters which had dissolved inorganic carbon (DIC) with low δ^{13} C values when compared to normal seawater. With

CONCLUSIONS

member.

The clumped isotope temperatures from Unda and San Salvador range between 20°C and 30°C, and Sr concentrations are typical of island dolomites with $\delta^{34}S$ values that are remof Plio-Pleistocene iniscent seawater.

may also be forming along the path, its contri-

bution to the δ^{13} C value of the carbonate is

small and therefore its influence is not evident

in the calculated $\delta^{13}C$ value of the calcite end

contrast, the clumped isotope temperatures from Clino range between 20°C and 50°C and bulk sediment δ^{34} S values suggest that portions of the dolomites formed from fluids that had undergone extensive bacterial sulphate reduction. In the upper portion of the core which has been influenced by meteoric and marine diagenesis, the clumped isotope values from the Clino core follow the geothermal gradient. However, in the regions that have been influenced by bacterial sulphate reduction (BSR), a disequilibrium occurs in Δ_{47} values with calculated temperatures being lower than expected.

A mixture of open system and closed system diagenesis is proposed. An open system is supported by marine δ³⁴S values and Sr concentrations, while a closed system is indicated by elevated δ³⁴S values, Sr concentrations and nonequilibrium Δ_{47} values. This interpretation is consistent with $\delta^{44/40}$ Ca values being elevated close to non-depositional surfaces, reflecting continuous replenishment of Ca from seawater in pore fluids during dolomite formation. On the other hand, δ^{26} Mg values averaging -2.8% exhibit no significant differences between massive dolomites formed in an open system when compared to background dolomites formed under bacterial influence, implying that dolomite formation is not mechanistically dependent on sulphate reduction, or the metabolic activities of sulphate reducing bacteria in these settings. The stratigraphic variation in δ^{34} S values in carbonate associated sulphate (CAS) is linked to sea-level influenced changes in local diagenetic systems, rather than secular changes in the biogeochemical cycling of the oceanic S reservoir. Similar findings and cautions have been discussed previously in the literature for C isotope records of ocean C cycling in the Bahamas (Swart, 2008) and older marine sedimentary successions (Patterson & Walter, 1994; Holmden et al., 1998; Knauth & Kennedy, 2009; Derry, 2010; Holmden et al., 2012a; Husson et al., 2015). The similarity in background dolomite in Clino and massive replacive dolomite in Unda and San Salvador and primary high-Mg calcite (HMC), and background dolomite from Site 1131 off the coast of Australia, indicate that background dolomite may form from HMC in a closed system with an average δ^{26} Mg value indistinguishable from Bahamas average dolomite of -2.8%. Thus, Mg isotopes by themselves cannot determine the closed or open system origin of dolomite in the rock record. Other proxies such as $\delta^{44/40}$ Ca and carbonate associated

sulphate $\delta^{34}S$ values must be employed to discern this difference. On the other hand, the insensitivity to the details of its diagenetic origins would appear to make dolomite a good candidate for reconstructing the secular history of seawater $\delta^{26}Mg$ values over geological time, if it can be ascertained that the dolomite formed early in the diagenetic history of the deposit and at temperatures close to ambient earth surface temperatures.

ACKNOWLEDGEMENTS

This work was supported by ACS Grant PRF# 52863-ND2 and NSF OCE1635874 to PKS, the Stable Isotope Laboratory and the Center of Carbonate Research Comparative Sedimentology Laboratory at the University of Miami. The Clino and Unda cores were collected under NSF Grant OCE8917295 to PKS and R.N. Ginsburg. Funding for the MAT 253 was provided by NSF Grant EAR-0926503 to PKS. Additional support for this work was provided by NSF grants OCE1537727 and OCE1635874 to PKS. The paper benefitted from the comments of Ted Present, two anonymous reviewers and the editorial comments of Greta Mackenzie.

DATA AVAILABILITY STATEMENT

Data are included in Appendix S1.

REFERENCES

- Ahm, A.-S.C., Bjerrum, C.J., Blättler, C.L., Swart, P.K. and Higgins, J.A. (2018) Quantifying early marine diagenesis in shallow-water carbonate sediments. *Geochim. Cosmochim. Acta*, **236**, 140–159.
- Allan, J.R. and Matthews, R.K. (1982) Isotope signatures associated with early meteoric diagenesis. Sedimentology, 29, 797–817.
- Baker, P.A. (1985) Pore-water chemistry of carbonate-rich sediments, Lord Howe Rise, Southwest Pacific Ocean. *Init. Rep. Deep Sea Drilling Proj.*, **90**, 1249–1256.
- Baker, P.A. and Bloomer, S.H. (1987) The origin of celestite in deep-sea carbonate sediments. *Geochim. Cosmochim.* Acta, 52, 335–340.
- Baker, P.A., Gieskes, J.M. and Elderfield, H. (1982) Diagenesis of carbonates in deep-sea sediments; evidence from Sr/Ca ratios and interstitial dissolved Sr²⁺ data. *J. Sed. Petrol.*, **52**, 71–82.
- Beach, D.K. and Ginsburg, R.N. (1980) Facies succession of Pliocene-Pleistocene carbonates, Northwestern Great Bahama Bank. AAPG Bull., 64, 1634–1642.

- Bernasconi, S.M., Muller, I.A., Bergmann, K.D., Breitenbach, S.F.M., Fernandez, A., Hodell, D.A., Jaggi, M., Meckler, A.N., Millan, I. and Ziegler, M. (2018) Reducing uncertainties in carbonate clumped isotope analysis through consistent carbonate-based standardization. Geochem. Geophys. Geosyst., 19, 2895–2914.
- Betzler, C., Eberli, G.P., Zarkian, C. and Shipboard Scientific Party (2016) Proceedings of the Initial Results of Expedition 359, 359. IODP, College Station, TX.
- Blättler, C.L., Miller, N.R. and Higgins, J.A. (2015) Mg and Ca isotope signatures of authigenic dolomite in siliceous deep-sea sediments. *Earth Planet. Sci. Lett.*, **419**, 32–42.
- Bottrell, S.H. and Newton, R.J. (2006) Reconstruction of changes in global sulfur cycling from marine sulfate isotopes. *Earth-Sci. Rev.*, 75, 59–83.
- Brand, W.A., Assonov, S.S. and Coplen, T.B. (2010) Correction for the 17 O interference in $\delta(^{13}$ C) measurements when analyzing CO_2 with stable isotope mass spectrometry (IUPAC Technical Report)*. Pure Appl. Chem., **82**, 1719–1733.
- Budd, A.F. and Manfrino, C. (2001) Coral assemblages and reef environments in the Bahamas Drilling Project cores. In: Subsurface Geology of a Prograding Carbonate Platform Margin, Great Bahama Bank: Results of the Bahamas Drilling Project (Ed. Ginsburg, R.N.), SEPM, SEPM Special Publications, 70, 41–59.
- Burdett, J.W., Arthur, M.A. and Richardson, M. (1989) A Neogene seawater sulfur isotope age curve from calcareous pelagic microfossils. *Earth Planet. Sci. Lett.*, **94**, 189–198.
- Carder, E.A., Galy, A., McKenzie, J.A., Vasconcelos, C. and Elderfield, H. (2005) Magnesium isotopes in bacterial dolomites: A novel approach to the dolomite problem. Geochim. Cosmochim. Acta, 69, A213.
- Chen, X., Romaniello, S.J., Herrmann, A.D., Hardisty, D., Gill, B.C. and Anbar, A.D. (2018) Diagenetic effects on uranium isotope fractionation in carbonate sediments from the Bahamas. Geochim. Cosmochim. Acta, 237, 294–311.
- Craig, H. (1957) Isotopic standards for carbon and oxygen and correction factors for mass- spectrometric analysis of carbon dioxide. Geochim. Cosmochim. Acta, 12, 133–149.
- Daeron, M., Blamart, D., Peral, M. and Affek, H.P. (2016) Absolute isotopic abundance ratios and the accuracy of Delta(47) measurements. Chem. Geol., 442, 83–96.
- Davies, A.J. and John, C.M. (2018) The clumped (13C–18O) isotope composition of echinoid calcite: further evidence for "vital effects" in the clumped isotope proxy. *Geochim. Cosmochim. Acta*, 245, 172–189.
- Davies, P.J., McKenzie, J.A. and Palmer-Julson, A. (Eds) (1991) Proceeding of Ocean Drilling Program Initial Reports, 133. Ocean Drilling Program, College Station, TX.
- Dawans, J. and Swart, P.K. (1988) Textural and geochemical alternations in late Cenozoic Bahamian dolomites. Sedimentology, 35, 385–403.
- Defliese, W.F. and Lohmann, K.C. (2016) Evaluation of meteoric calcite cements as a proxy material for mass-47 clumped isotope thermometry. *Geochim. Cosmochim. Acta*, 173, 126–141.
- Defliese, W.F., Hren, M.T. and Lohmann, K.C. (2015) Compositional and temperature effects of phosphoric acid fractionation on Δ47 analysis and implications for discrepant calibrations. Chem. Geol., 396, 51–60.
- Dellinger, M., West, A.J., Planavsky, NoahJ., Hardisty, D., Gill, B.C., Kalderon-Asael, B., Asael, D., Croissant, T. and Swart, P.K. (2019) The effects of diagenesis on Li isotope

- ratios of shallow marine carbonates. Am. J. Sci., 320, 150-184.
- Dennis, K.J., Affek, H., Passey, B.H., Schrag, D.P. and Eiler, J.M. (2011) Defining an absolute reference frame for 'clumped' isotope studies of CO₂. Geochim. Cosmochim. Acta, 75, 7117–7131.
- Derry, L.A. (2010) On the significance of ¹³C correlations in ancient sediments. Earth Planet. Sci. Lett., 296, 497–501.
- van Dijk, I., Barras, C., de Nooijer, L.J., Mouret, A., Geerken, E., Oron, S. and Reichart, G.J. (2019) Coupled calcium and inorganic carbon uptake suggested by magnesium and sulfur incorporation in foraminiferal calcite. *Biogeosciences*, 16, 2115–2130.
- Eberli, G.P. (2000) The record of Neogene sea-level changes in the prograding carbonates along the Bahamas transect-Leg 166 synthesis. In: *Proceedings of the Ocean Drilling Program, Scientific Results* (Eds Swart, P.K., Eberli, G.P., Malone, M.J. and Sarg, J.F.), 166, 167–177.
- Eberli, G.P., Swart, P.K. and Malone, M.J. (Eds) (1997a)

 Proceedings of Ocean Drilling Program Initial Reports,
 166. Ocean Drilling Program, College Station, TX.
- Eberli, G.P., Swart, P.K., McNeill, D.F., Kenter, J.A.M., Anselmetti, F.S., Melim, L.A. and Ginsburg, R.N. (1997b) A synopsis of the bahamas drilling project: results from two deep core borings drilled on the Great Bahama Bank. In: Proceedings of the Ocean Drilling Program, Initial Reports, 166.
- Fantle, M.S. and DePaolo, D.J. (2007) Ca isotopes in carbonate sediment and pore fluid from ODP Site 807A: The Ca²⁺(aq)-calcite equilibrium fractionation factor and calcite recrystallization rates in Pleistocene sediments. Geochim. Cosmochim. Acta, 71, 2524–2546.
- Fantle, M.S. and Higgins, J. (2014) The effects of diagenesis and dolomitization on Ca and Mg isotopes in marine platform carbonates: implications for the geochemical cycles of Ca and Mg. *Geochim. Cosmochim. Acta*, 142, 458–481.
- Farkas, J., Boehm, F., Wallmann, K., Blenkinsop, J., Eisenhauer, A., van Geldern, R., Munnecke, A., Voigt, S. and Veizer, J. (2007) Calcium isotope record of Phanerozoic oceans: implications for chemical evolution of seawater and its causative mechanisms. Geochim. Cosmochim. Acta, 71, 5117-5134.
- Feary, D.A., Hine, A.C. and Malone, M. (Eds) (1998) Proceeding of the Ocean Drilling Program, Initial Results. Ocean Drilling Program, College Station, TX.
- Fry, B., Silva, S.R., Kendall, C. and Anderson, R.K. (2002) Oxygen isotope corrections for online δ^{34} S analysis. *Rapid Commun. Mass Spectrom.*, **16**, 854–858.
- Galy, A., Belshaw, N.S., Halicz, L. and O'Nions, R.K. (2001) High-precision measurements of magnesium isotopes by multiple-collector inductively coupled plasma mass spectrometry. *Int. J. Mass Spectrom.*, 89–98.
- Gieskes, J.M., Elderfield, H. and Palmer, M.R. (1986) Strontium and its isotopic composition in interstitial waters of marine carbonate sediments. *Earth Planet. Sci. Lett.*, 77, 229–235.
- Gill, B.C., Lyons, T.W. and Frank, T.D. (2008) Behavior of carbonate-associated sulfate during meteoric diagenesis and implications for the sulfur isotope paleoproxy. *Geochim. Cosmochim. Acta*, 72, 4699–4711.
- Gill, B.C., Lyons, T.W., Young, S.A., Kump, L.R., Knoll, A.H. and Saltzman, M.R. (2011) Geochemical evidence for widespread euxinia in the Later Cambrian ocean. *Nature*, 469, 80–83.

- Ginsburg, R.N. (2001) The Bahamas drilling project: background and acquisition of cores and logs. In: Subsurface Geology of a Prograding Carbonate Platform Margin Great Bahama Bank Results of the Bahamas Drilling Project (Ed. Ginsburg, R.N.), 70, pp. 3–13. Society of Economic Paleontologists and Mineralogists Special publication, Tulsa, OK.
- Guzikowski, M. (1987) Evolution of pore fluid chemistry during recrystallization of periplatfrom carbonates, Bahamas. University of Miami, Miami, FL, 215 pp.
- Hardisty, D.S., Lu, Z., Bekker, A., Diamond, C.W., Gill, B.C.,
 Jiang, G., Kah, L.C., Knoll, A.H., Loyd, S.J., Osburn, M.R.,
 Planavsky, N.J., Wang, C., Zhou, X. and Lyons, T.W.
 (2017) Perspectives on Proterozoic surface ocean redox
 from iodine contents in ancient and recent carbonate.
 Earth Planet. Sci. Lett., 463, 159–170.
- He, B., Olack, G.A. and Colman, A.S. (2012) Pressure baseline correction and high-precision CO_2 clumpedisotope (Δ_{47}) measurements in bellows and microvolume modes. Rapid Commun. Mass Spectrom., 26, 2837–2853.
- Higgins, J.A. and Schrag, D.P. (2012) Records of Neogene seawater chemistry and diagenesis in deep-sea carbonate sediments and pore fluids. *Earth Planet. Sci. Lett.*, 357, 386–396.
- Higgins, J., Blättler, C.L., Lundstrom, E.A., Santiago-Ramos,
 D.P., Akhtar, A.A., Crüger-Ahm, A.S., Bialik, O.,
 Holmden, C., Bradbury, H., Murray, S.T. and Swart, P.K.
 (2018) Mineralogy, early marine diagenesis and the chemistry of shallow water carbonate sediments. Geochim. Cosmochim. Acta, 220, 512–534.
- Holmden, C., Creaser, R.A., Muehlenbachs, K., Leslie, S.A. and Bergstrom, S.M. (1998) Isotopic evidence for geochemical decoupling between ancient epeiric seas and bordering oceans: Implications for secular curves. Geology, 26, 567–570.
- Holmden, C., Panchuk, K. and Finney, S.C. (2012) Tightly coupled records of Ca and C isotope changes during the Hirnantian glaciation event in an epeiric sea setting. Geochim. Cosmochim. Acta, 98, 94–106.
- Holmden, C., Papanastassiou, D.A., Blanchon, P. and Evans, S. (2012) Delta Ca-44/40 variability in shallow water carbonates and the impact of submarine groundwater discharge on Ca-cycling in marine environments. Geochim. Cosmochim. Acta, 83, 179–194.
- Horita, J. (2014) Oxygen and carbon isotope fractionation in the system dolomite-water-CO₂ to elevated temperatures. Geochim. Cosmochim. Acta, 129, 111-124.
- Huntington, K.W., Eiler, J.M., Affek, H., Guo, W., Bonifacie, M., Yeung, L.Y., Thiagarajan, N., Passey, B.H., Tripati, A.K., Daëron, M. and Came, R. (2009) Methods and limitations of 'clumped' CO₂ isotope (Δ₄₇) analysis by gassource isotope ratio mass spectrometry. *J. Mass Spectrom.*, 44, 1318–1329.
- Husson, J.M., Higgins, J.A., Maloof, A.C. and Schoene, B. (2015) Ca and Mg isotope constraints on the origin of Earth's deepest δ^{13} C excursion. *Geochim. Cosmochim. Acta*, **160**, 243–266.
- **Jacobson, A.D.** and **Holmden, C.** (2008) δ^{44} Ca evolution in a carbonate aquifer and its bearing on the equilibrium isotope fractionation factor for calcite. *Earth Planet. Sci. Lett.*, **270**, 349–353.
- Kaldi, J. and Gidman, J. (1982) Early diagenetic dolomitic cements-Examples from the Permian lower Magensian

- Limestone of England and the Pleistocene carbonates of the Bahamas. *J. Sediment. Petrol.*, **52**, 1073–1085.
- Kampschulte, A. and Strauss, H. (2004) The sulfur isotopic evolution of Phanerozoic seawater based on the analysis of structurally substituted sulfate in carbonates. *Chem. Geol.*, 204, 255–286.
- Kaplan, I.R. and Rittenberg, S.C. (1964) Microbiological fraction of sulphur isotopes. J. Gen. Microbiol., 34, 195–212.
- Kelts, K. and McKenzie, J.A. (1982) Diagenetic dolomite formation in Quaternary anoxic diatomaceous muds of Deep Sea Drilling Project Leg 64, Gulf of California. *Init. Rep. Deep Sea Drilling Proj.*, 64, 553–569.
- Kenter, J.A.M., Ginsburg, R.N. and Troelstra, S.R. (2001) Sea-level-driven sedimentation patterns on the slope and margin. In: Subsurface Geology of a prograding carbonate platform margin, Great Bahama Bank: Results of the Bahamas Drilling Project (Ed. Ginsburg, R.N.), SEPM Special Publication, 70, 61–100. Society of Economic Paleontologists and Mineralogists, Tulsa, OK.
- Kievman, C.M. (1996) Sea-level effects on carbonate platform evolution: Plio-Pleistocene Northwestern Great Bahama Bank. University of Miami, FL, 245 pp.
- Kievman, C.M. (1998) Match between late Pleistocene Great Bahama Bank and deep-sea oxygen isotope records of sea level. Geology, 26, 635–638.
- Kim, S.-T. and O'Neil, J.R. (1997) Equilibrium and nonequilibrium oxygen isotope effects in synthetic carbonates. Geochim. Cosmochim. Acta, 61, 3461–3475.
- **Kimmig, S.R.** and **Holmden, C.** (2017) Multi-proxy geochemical evidence for primary aragonite precipitation in a tropical-shelf 'calcite sea' during the Hirnantian glaciation. *Geochim. Cosmochim. Acta*, **206**, 254–272.
- Knauth, L.P. and Kennedy, M.J. (2009) The late Precambrian greening of the Earth. Nature, 460, 728–732.
- Kramer, P.A., Swart, P.K., De Carlo, E.H. and Schovsbo,
 N.H. (2000) Overview of Leg 166 interstitial fluid and sediment geochemistry, Sites 1003–1007 (Bahamas Transect). In: Proceedings of the Ocean Drilling Program, Scientific Results (Eds Swart, P.K., Eberli, G.P. and Malone, M.), 166, pp. 179–198. Ocean Drilling Program, College Station, TX.
- Land, L.S. (1980) The isotopic and trace element geochemistry of dolomite: the state of the art. In: Concepts and Models of Dolomitization (Eds Zenger, D.H., Dunham, J.B. and Ethington, R.L.), Society of Economic Paleontologists and Mineralogists Special publication, Tulsa, 28, 87–110.
- Lawrence, J.R., Gieskes, J.M. and Broecker, W.S. (1975) Oxygen isotope and cation composition of DSDP pore waters and alteration of Layer-II basalts. *Earth Planet. Sci.* Lett., 27, 1–10.
- Li, Y.H. and Gregory, S. (1974) Diffusion of ions in seawater and in deep sea sediments. Geochim. Cosmochim. Acta, 38, 703–714.
- **Lisiecki, L.E.** and **Raymo**, **M.E.** (2005) A Pliocene-Pleistocene stack of 57 globally distributed benthic δ^{18} O records. *Paleoceanography*, **20**, 1–17.
- Liu, X.-M., Hardisty, D.S., Lyons, T.W. and Swart, P.K. (2019) Evaluating the fidelity of the cerium paleoredox tracer during variable carbonate diagenesis on the Great Bahamas Bank. Geochim. Cosmochim. Acta, 248, 25–42.
- Loyd, S.J., Corsetti, F.A., Eiler, J.M. and Tripati, A.K. (2012)

 Determining the diagenetic conditions of concretion

- formation: Assessing temperatures and pore water using clumped isotopes. J. Sed. Res., 82, 1006–1016.
- Loyd, S.J., Sample, J., Tripati, R.E., Defliese, W.F., Brooks, K., Hovland, M., Torres, M., Marlow, J., Hancock, L.G., Martin, R., Lyons, T. and Tripati, A.E. (2016) Methane seep carbonates yield clumped isotope signatures out of equilibrium with formation temperatures. *Nat. Commun.*, 7, 1–12.
- Lyons, T.W., Hurtgen, M.T. and Gill, B.C. (2005) New insight into the utility of carbonate-associated sulfate. Geochim. Cosmochim. Acta, 69, A128.
- Manfrino, C.M. and Ginsburg, R.N. (2001) Pliocene to Pleistocene depositional history of the Upper Platform Margin. In: Subsurface Geology of a Prograding Carbonate Platform Margin, Great Bahama Bank: Results of the Bahama Drilling Project (Ed. Ginsburg, R.), 70, pp. 17–39. Society of Economic Paleontologists and Mineralogists, Tulsa, OK.
- Marenco, P.J., Corsetti, F.A., Kaufman, A.J. and Bottjer, D.J. (2008) Environmental and diagenetic variations in carbonate associated sulfate: An investigation of CAS in the Lower Triassic of the western USA. Geochim. Cosmochim. Acta, 72, 1570–1582.
- Matthews, A. and Katz, A. (1977) Oxygen isotope fractionation during the dolomitization of calcium carbonate. *Geochim. Cosmochim. Acta*, 41, 1431–38.
- McNeill, D.F., Ginsburg, R.N., Chang, S.-B.R. and Kirschvink, J.L. (1988) Magnetostratigraphic dating of shallow-water carbonates from San Salvador Bahamas. *Geology*, **16**, 8–12.
- McNeill, D.F., Eberli, G.P., Lidz, B., Swart, P.K. and Kenter, J.A.M. (2001) Chronostratigraphy of a prograded carbonate platform margin: a record of dynamic slope sedimentation, western Great Bahama Bank. In: Subsurface Geology of a Prograding Carbonate Platform Margin, Great Bahama Bank: Results of the Bahamas Drilling Project (Ed. Ginsburg, R.N.), pp. 101–134. SEPM (Society for Sedimentary Geology), Tulsa, OK.
- Melim, L.A., Swart, P.K. and Maliva, R.G. (1995) Meteoriclike fabrics forming in marine waters: Implications for the use of petrography to identify diagenetic environments. *Geology*, **23**, 755–758.
- Melim, L.A., Swart, P.K. and Maliva, R.G. (2001) Meteoric and marine-burial diagenesis in the subsurface of Great Bahama Bank. In: Subsurface Geology of a Prograding Carbonate Platform Margin, Great Bahama Bank: Results of the Bahama Drilling Project (Ed. Ginsburg, R.N.), SEPM Special Publication, 70, pp. 137–161. Society of Economic Paleontologists and Mineralogists, Tulsa, OK.
- Melim, L.A., Swart, P.K. and Eberli, G.P. (2004) Mixing-zone diagenesis in the subsurface of Florida and The Bahamas. J. Sed. Res., 74, 904–913.
- Müller, I.A., Violay, M.E.S., Storck, J.-C., Fernandez, A., Dijk, J.V., Madonna, C. and Bernasconi, S.M. (2016) Clumped isotope fractionation during phosphoric acid digestion of carbonates at 70 C. Chem. Geol., 449, 1–14.
- Mullins, H.T., Wise, S.W., Land, L.S., Siegel, D.I., Masters, P.M., Hinchey, E.J. and Price, K.R. (1985) Authigenic dolomite in Bahamian peri-platform slope sediment. *Geology*, 13, 292–295.
- Mullins, H.T., Gardulski, A.F., Hinchey, E.J. and Hine, A.C. (1988) The modern carbonate ramp slope of central west Florida. *I. Sed. Petrol.*, 58, 273–290.
- Murphy, J.G., Swart, P.K. and Higgins, J.A. (2018) Assessing the effects of early marine diagenesis on the lithium

- isotopic composition of shallow marine carbonate. In: *AGU Abstracts*, PP41E-1893. AGU, Washington, DC.
- Murray, S.T. and Swart, P.K. (2017) Evaluating formation fluid models and calibrations using clumped isotope paleothermometry on Bahamian dolomites. *Geochim. Cosmochim. Acta*, **206**, 73–93.
- Murray, S.T., Arienzo, M.M. and Swart, P.K. (2016) Determining the Δ_{47} acid fractionation in dolomites. Geochim. Cosmochim. Acta, 174, 42–53.
- Nagihara, S. and Wang, K. (2000) Geothermal regime of the Western margin of the Great Bahama Bank. In: Proceedings of the Ocean Drilling Program (Eds Swart, P.K., Eberli, G.P., Malone, M.J. and Sarg, J.F.), 166, pp. 113–120. ODP, College Station, TX.
- Oehlert, A.M. and Swart, P.K. (2014) Interpreting carbonate and organic carbon isotope covariance in the sedimentary record. *Nature. Communications*, 5.
- **Oehlert, A.** and **Swart, P.K.** (2019) Rolling window regression of δ^{13} C and δ^{18} O values in carbonate sediments: implications for source and diagenesis. *Depos. Rec.*, **5**, 613–630.
- Patterson, W.P. and Walter, L.M. (1994) Depletion in 13 C in seawater CO_2 on modern carbonate platforms: significance for the carbon isotopic record of carbonate. *Geology*, 22, 885–888.
- Paytan, A., Kastner, M., Campbell, D. and Thiemens, M.H. (1998) Sulfur isotopic composition of Cenozoic seawater sulfate. Science, 282, 1459-1462.
- Paytan, A., Kastner, M., Campbell, D. and Thiemens, M.H. (2004) Seawater sulfur isotope fluctuations in the cretaceous. Science, 304, 1663–1665.
- Pierson, B.J. (1983) Cyclic sedimentation, limestone diagenesis and dolomitization in Upper Cenozoic carbonates of the Southeastern Bahamas. Dissertation, University of Miami, 343 pp.
- Present, T.M., Paris, G., Burke, A., Fischer, W.W. and Adkins, J.F. (2015) Large carbonate associated sulfate isotopic variability between brachiopods, micrite and other sedimentary components in Late Ordovician strata. *Earth Planet. Sci. Lett.*, 432, 187–198.
- Present, T.M., Gutierrez, M., Paris, G., Kerans, C., Grotzinger, J.P. and Adkins, J.F. (2019) Diagenetic controls on the isotopic composition of carbonateassociated sulphate in the Permian Capitan Reef Complex, West Texas. Sedimentology, 66, 2605–2626.
- Reijmer, J.J.G., Swart, P.K., Bauch, T., Otto, R., Roth, S. and Zechel, S. (2009) A reevaluation of facies on Great Bahama Bank I: new facies maps of Western Great Bahama Bank. In: Perspectives in Carbonate Geology: A Tribute to the Career of Robert Nathan Ginsburg, IAS Special Publication (Eds Swart, P.K., Eberli, G.P. and McKenzie, J.A.), 41, pp. 29–46. Wiley-Blackwell, Oxford.
- Rennie, V.C.F. and Turchyn, A.V. (2014) The preservation of delta S-34(SO4) and delta O-18(SO4) in carbonate-associated sulfate during marine diagenesis: a 25 Myr test case using marine sediments. *Earth Planet. Sci. Lett.*, **395**, 12, 22
- Rivers, J.M., Kyser, T.K. and James, N.P. (2012) Salinity reflux and dolomitization of southern Australian slope sediments: the importance of low carbonate saturation levels. *Sedimentology*, **59**, 445–465.
- Rosenbaum, J. and Sheppard, S.M.F. (1986) An isotopic study of siderites, dolomites and ankerites at higtemperatures. *Geochim. Cosmochim. Acta*, **50**, 1147–1150.

- Saenger, C. and Wang, Z. (2014) Magnesium isotope fractionation in biogenic and abiogenic carbonates: implications for paleoenvironmental proxies. *Quatern. Sci. Rev.*, 90, 1–21.
- Saenger, C., Affek, H.P., Felis, T., Thiagarajan, N., Lough, J.M. and Holcomb, M. (2012) Carbonate clumped isotope variability in shallow water corals: temperature dependence and growth-related vital effects. *Geochim. Cosmochim. Acta*, 99, 224–242.
- Schauer, A.J., Kelson, J., Saenger, C. and Huntington, K.W. (2016) Choice of $^{17}{\rm O}$ correction affects clumped isotope (Δ_{47}) values of CO₂ measured with mass spectrometry. Rapid Commun. Mass Spectrom., 24, 2607–2616.
- Sharma, T. and Clayton, R.N. (1965) Measurement of ¹⁸O/ ¹⁶O ratios of total oxygen of carbonates. Geochim. Cosmochim. Acta, 29, 1347–1353.
- Shinn, E.A., Lloyd, R.M. and Ginsburg, R.N. (1969) Anatomy of a modern carbonate tidal-flat andros Island, Bahamas. J. Sed. Petrol., 39, 1202–1228.
- Staudigel, P.T. and Swart, P.K. (2019) A diagenetic origin for isotopic variability of sediments deposited on the margin of Great Bahama Bank, insights from clumped isotopes. *Geochim. Cosmochim. Acta*, **258**, 97–119.
- Staudigel, P.T., Murray, S., Dunham, D., Frank, T., Fielding, C.R. and Swart, P.K. (2018) Cryogenic brines as diagenetic fluids: reconstructing the alteration history of the Victoria Land Basin using clumped isotopes. *Geochim. Cosmochim. Acta*, 224, 154–170.
- Strauss, H. (1997) The isotopic composition of sedimentary sulfur through time. Palaeogeogr. Palaeoclimatol. Palaeoecol., 132, 97–118.
- Supko, P.R. (1977) Subsurface dolomites, San Salvador, Bahamas. J. Sed. Petrol., 47, 1063–1077.
- Swart, P.K. (1988) The elucidation of dolomitization events using nuclear-track mapping. In: Sedimentology and Geochemistry of Dolostones (Eds Shukla, E.V. and Baker, P.A.), 43, pp. 11–24. Society of Economic Paleontologists and Mineralogists, Tulsa, OK.
- Swart, P.K. (2000) The oxygen isotopic composition of interstitial waters: evidence for fluid flow and recrystallization in the margin of Great Bahama Bank. In: Proceedings of the Ocean Drilling Program, Scientific Results (Eds Swart, P.K., Eberli, G.P. and Malone, M.), 166, pp. 91–98. College Station, TX.
- Swart, P.K. (2008) Global synchronous changes in the carbon isotopic composition of carbonate sediments unrelated to changes in the global carbon cycle. *Proc. Natl. Acad. Sci.* USA, 105, 13741–13745.
- Swart, P.K. (2015) The geochemistry of carbonate diagenesis: The past, present and future. Sedimentology, 62, 1233–1304.
- **Swart, P.K.** and **Kennedy, M.J.** (2012) Does the global stratigraphic reproducibility of δ^{13} C in Neoproterozoic carbonates require a marine origin? A Pliocene-Pleistocene comparison. *Geology*, **40**, 87–90.
- Swart, P.K. and Melim, L.A. (2000) The origin of dolomites in tertiary sediments from the margin of Great Bahama Bank. J. Sed. Res., 70, 738–748.
- Swart, P.K. and Oehlert, A.M. (2019) Revised interpretations of stable C and O patterns in carbonate rocks resulting from meteoric diagenesis. Sed. Geol., 364, 14–23.
- Swart, P.K., Ruiz, J. and Holmes, C.W. (1987) Use of strontium isotopes to constrain the timing and mode of dolomitization of Upper Cenozoic sediments in a core from San Salvador, Bahamas. *Geology*, **15**, 262–265.

- Swart, P.K., Burns, S.J. and Leder, J.J. (1991) Fractionation of the stable isotopes of oxygen and carbon in carbon dioxide during the reaction of calcite with phosphoric acid as a function of temperature and technique. *Chem. Geol.*, **86**, 89–96.
- Swart, P.K., Elderfield, H. and Beets, K. (2001) The ⁸⁷Sr/⁸⁶Sr ratios of carbonates, phosphorites and fluids collected during the Bahamas Drilling Project. In: Subsurface gology of a prograding carbonate platform margin, Great Bahama Bank: Results of the Bahams Drilling Project (Ed. Ginsburg, R.N.), 70. SPEM, Tulsa, OK.
- Swart, P.K., James, N.P., Mallinson, D., Malone, M.J., Matsuda, H. and Simo, T. (2002) Data report: carbonate mineralogy of sites Drilled during Leg 182. In: Proceedings of the Ocean Drilling Program Scientific Results (Eds Feary, D.A., Hine, A.C. and Malone, M.J.), 182. Ocean Drilling Program, College Station, TX.
- Swart, P.K., Reijmer, J.J. and Otto, R. (2009) A reevaluation of facies on Great Bahama Bank II: variations in the δ¹³C, δ¹⁸O and mineralogy of surface sediments. In: Perspectives in Carbonate Geology: A Tribute to the Career of Robert Nathan Ginsburg, IAS Special Publication (Eds Swart, P.K., Eberli, G.P. and McKenzie, J.A.), 41, pp. 47–60. Wiley-Blackwell, Oxford.
- Swart, P.K., Murray, S.T., Staudigel, P.T. and Hodell, D.A. (2019) Oxygen isotopic exchange between CO₂ and phosphoric acid: implications for the measurement of clumped isotopes in carbonates. *Geochem., Geophys. Geosyst.*, **20**, 1–21.
- Tissot, F.L.H., Chen, C., Go, B.M., Naziemiec, M., Healy, G., Bekker, A., Swart, P.K. and Dauphas, N. (2018) Controls of eustasy and diagenesis on the ²³⁸U/²³⁵U of carbonates and evolution of the seawater (²³⁴U/²³⁸U) during the last 1.4 Myr. *Geochim. Cosmochim. Acta*, **242**, 233–265.
- Turchyn, A.V. and DePaolo, D.J. (2011) Calcium isotope evidence for suppression of carbonate dissolution in carbonate-bearing organic-rich sediments. Geochim. Cosmochim. Acta, 75, 7081–7098.
- Vahrenkamp, V.C. (1988) Constraints on the formation of platform dolomites: a geochemical study of late tertiary dolomite from Little Bahama Bank, Bahamas. Dissertation, University of Miami, 434 pp.

- Vahrenkamp, V.C. and Swart, P.K. (1990) New distribution coefficient for the incorporation of strontium into dolomite and its implications for the formation of ancient dolomites. *Geology*, **18**, 387–391.
- Vahrenkamp, V.C. and Swart, P.K. (1994) Late Cenozoic dolomites of the Bahamas: metastable analogues for the genesis of ancient platform dolomites. In: *Dolomieu Conference on Carbonate Platforms and Dolomitization* (Eds Purser, B.H., Tucker, M.E. and Zenger, D.H.), 21, pp. 133–153. Blackwell, Oxford.
- Vahrenkamp, V.C., Swart, P.K. and Ruiz, J. (1991) Episodic dolomitization of Late Cenozoic carbonates in the Bahamas – evidence from strontium isotopes. J. Sed. Petrol., 61, 1002–1014.
- Vasconcelos, C. and McKenzie, J.A. (1997) Microbial mediation of modern dolomite precipitation and diagenesis under anoxic conditions (Lagoa Vermelha, Rio de Janeiro, Brazil). J. Sed. Res., 67, 378–390.
- Warthmann, R., Van Lith, Y., Vasconcelos, C., McKenzie, J.A. and Karpoff, A.M. (2000) Bacterially induced dolomite precipitation in anoxic culture experiments. *Geology*, **28**, 1091–1094.
- Wortmann, U.G., Bernasconi, S.M. and Böttcher, M.E. (2001) Hypersulfidic deep biosphere indicates extreme sulfur isotope fractionation during single-step microbial sulfate reduction. *Geology*, 29, 647–650.

Manuscript received 21 July 2019; revision 8 June 2020; revision accepted 12 June 2020

Supporting Information

Additional information may be found in the online version of this article:

Appendix S1. Supplemental Information for the elucidation of dolomitization in deep water Bahamian sediments using sulphur, calcium, magnesium and clumped isotopes.